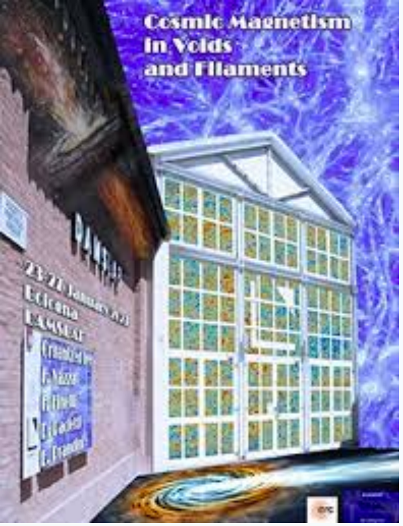

Messengers from the Early Universe: Magnetic Fields, Turbulence, and Gravitational Waves

Tina Kahniashvili
Carnegie Mellon University (USA)
Ilia State University (Georgia)

Cosmic Magnetism in Voids and Filaments
January 24, 2023

outline

- looking backward – Cauchy's problem
- big bang nucleosynthesis
- cosmic microwave background
- gravitational waves

Based on:

- Brandenburg, Clarke, Kahniashvili, Long, Sun, *work in progress*
- Kahniashvili, Clarke, Stepp, Brandenburg. PRL 128, 221301 (2022)
- Roper Pol, Mandal, Brandenburg, Kahniashvili, JCAP 04, 019 (2022)
- Brandenburg, Gogoberidze, Kahniashvili, Mandal, Roper Pol, Shenoy, Class. Quant. Grav. 38, 145002 (2021)
- Brandenburg, Clarke, He, Kahniashvili, PRD 104, 043513 (2021)
- Brandenburg, He, Kahniashvili, Rheinhardt, Schober, ApJ 911, 110, (2021)
- Kahniashvili, Brandenburg, Gogoberidze, Mandal, Roper Pol, PRR 3, 113193 (2021)
- Roper Pol, Mandal, Brandenburg, Kahniashvili, Kosowsky, PRD 102, 083512 (2020)

Brief History of the Universe

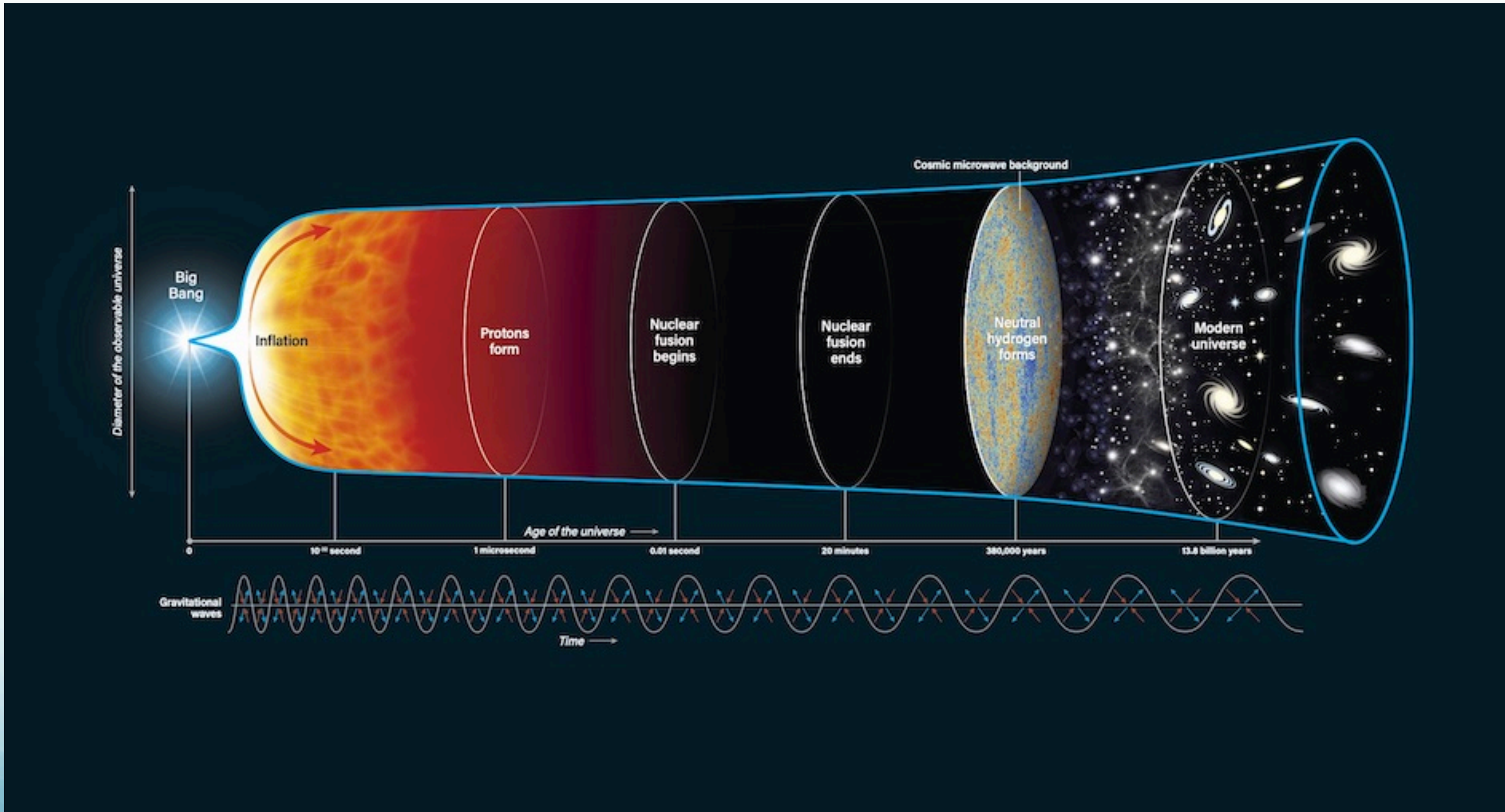

https://astronomy.com/magazine/news/2021/01/the-beginning-to-the-end-of-the-universe-inflating-the-universe

Cauchy Problem at Work

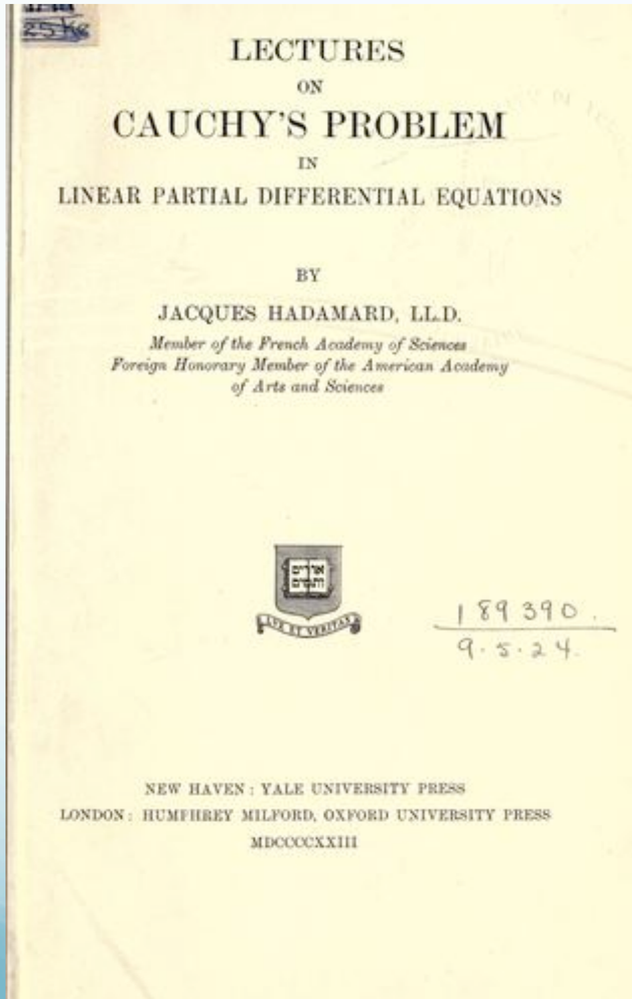
LECTURES

ON

CAUCHY'S PROBLEM

IN

LINEAR PARTIAL DIFFERENTIAL EQUATIONS

BY

JACQUES HADAMARD, LL.D.

Member of the French Academy of Sciences
Foreign Honorary Member of the American Academy
of Arts and Sciences

189390.
9.5.24.

NEW HAVEN : YALE UNIVERSITY PRESS
LONDON : HUMPHREY MILFORD, OXFORD UNIVERSITY PRESS
MDCCCCXXIII

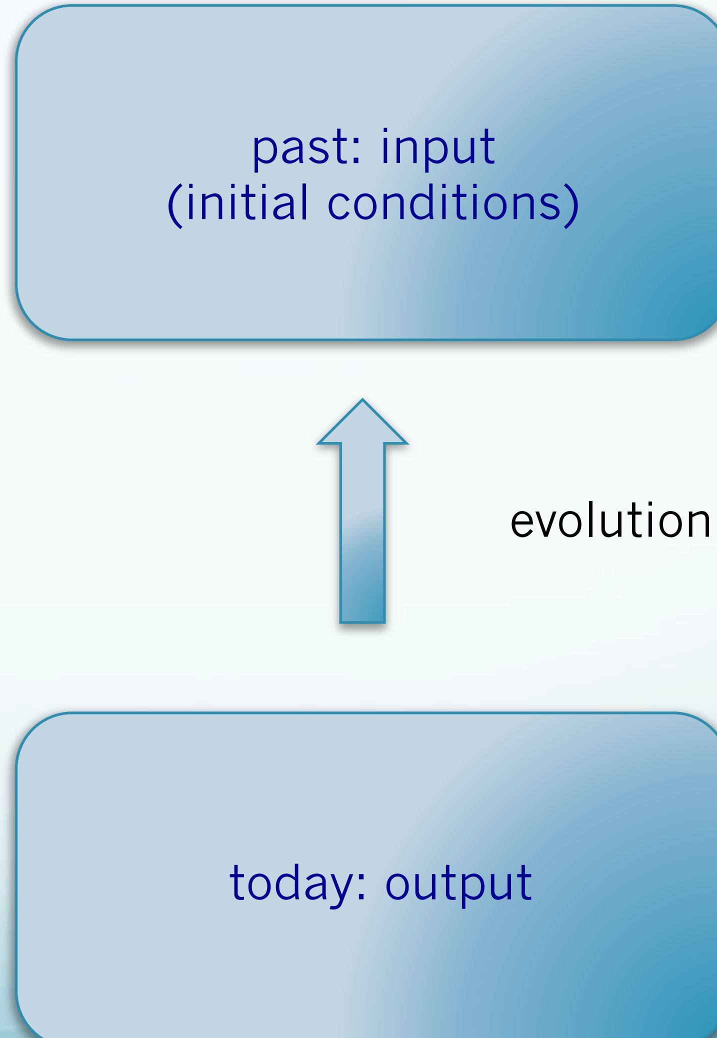

Today: Cosmic Magnetism

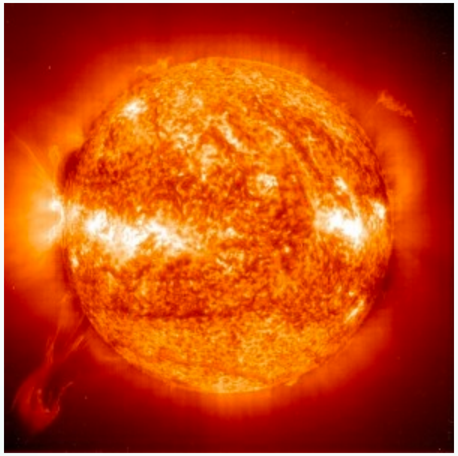

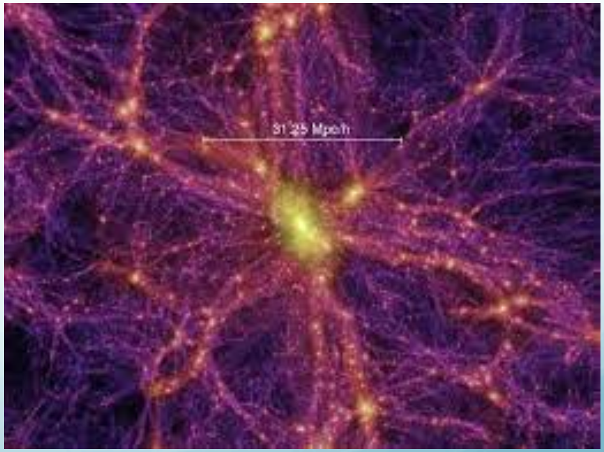

Cosmic Magnetic Fields

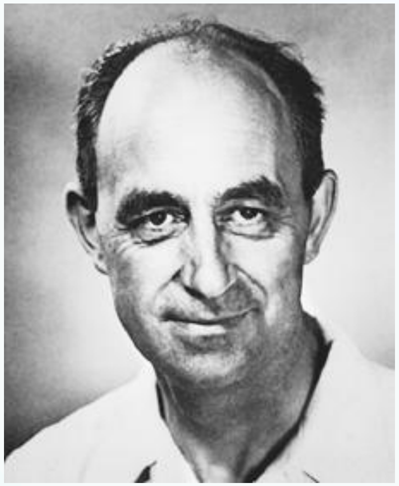

E. Fermi
***"On the origin of the cosmic radiation"*,**
PRD, 75, 1169 (1949)

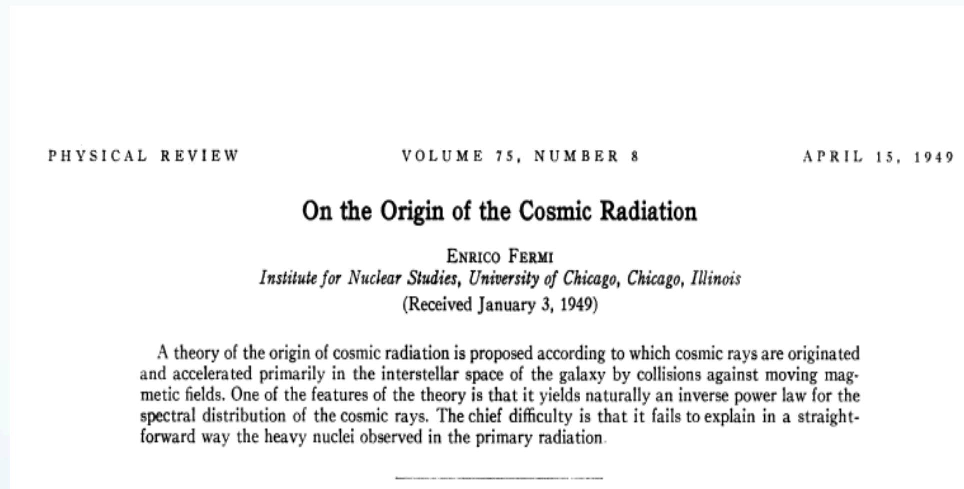

PHYSICAL REVIEW VOLUME 75, NUMBER 8 APRIL 15, 1949

On the Origin of the Cosmic Radiation

ENRICO FERMI
Institute for Nuclear Studies, University of Chicago, Chicago, Illinois
(Received January 3, 1949)

A theory of the origin of cosmic radiation is proposed according to which cosmic rays are originated and accelerated primarily in the interstellar space of the galaxy by collisions against moving magnetic fields. One of the features of the theory is that it yields naturally an inverse power law for the spectral distribution of the cosmic rays. The chief difficulty is that it fails to explain in a straightforward way the heavy nuclei observed in the primary radiation.

https://phys.org/news/2011-05-cosmic-magnetic-fields.html

Blazars Spectra Observations:

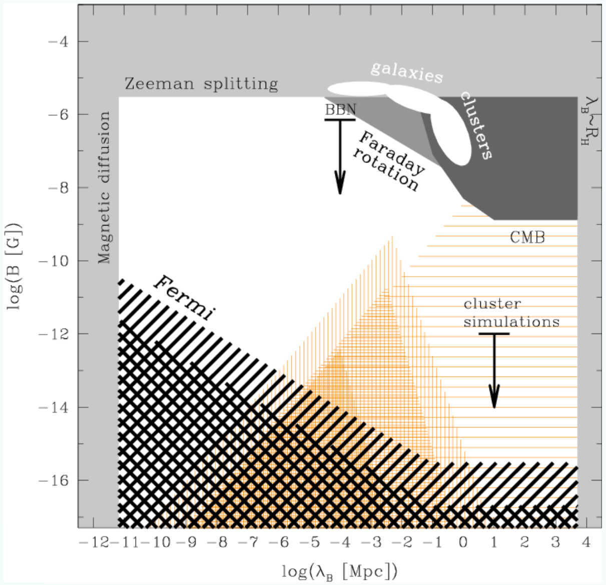

A. Neronov & E. Vovk,*" Evidence for Strong Extra-galactic Magnetic Fields from Fermi Observations of TeV Blazars*", Science 328, 5974 (2010)

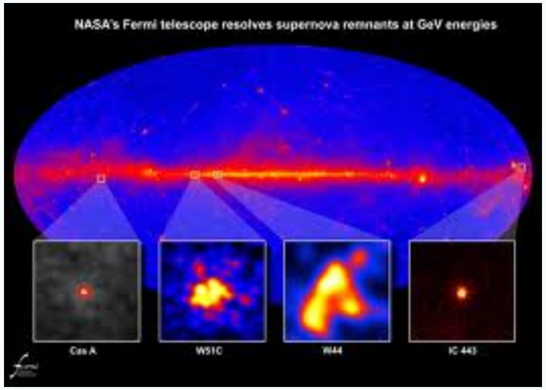

V. A. Acciari et al. [MAGIC Collaboration] *"A Lower Bound on Intergalactic Magnetic Fields from Time Variability of 1ES 0229+200 from MAGIC and Fermi/LAT Observations"* arXiv: 2210.03321

S. Archambault et al. [VERITAS Collaboration], *"Search for Magnetically Broadened Cascade Emission From Blazars with VERITAS,"* Astrophys. J. 835 , 288 (2017).

M. Ackermann, et al. [Fermi-LAT Collaboration], *"The Search for Spatial Extension in High-latitude Sources Detected by the Fermi Large Area Telescope,"* Astrophys. J. Suppl. 237 , 32 (2018).

Two Scenarios

- **Astrophysical Scenario(s)**
  - The seed is typically very weak and the magnetic field is transferred from local sources within galaxies to large scales

Ejection

Primordial

z=4

z=0

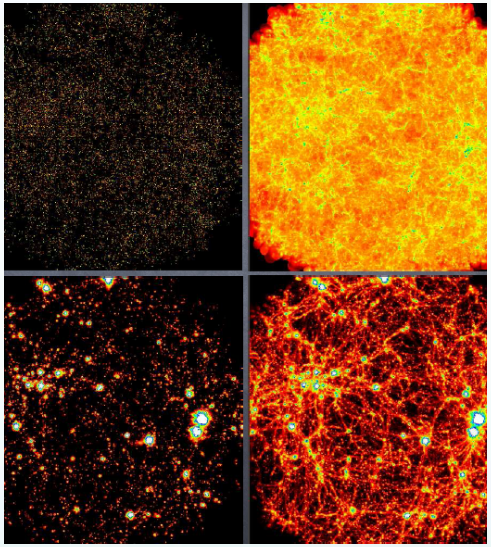

z=4

z=0

Donnert et al. 2008

- **Cosmological Scenario(s)**
  - The seed is generated prior to galaxy formation in the early universe on scales that are large now

Primordial or Astrophysical Origin?

E ASTROPHYSICAL JOURNAL LETTERS, 727:L4 (4pp), 2011 January 20 doi:10.1088/2041-8205/727/1/L4

LOWER LIMIT ON THE STRENGTH AND FILLING FACTOR OF EXTRAGALACTIC MAGNETIC FIELDS

K. DOLAG[1,2], M. KACHELRIESS[3], S. OSTAPCHENKO[3,4], AND R. TOMÀS[5]
[1] Universitätssternwarte München, München, Germany
[2] Max-Planck-Institut für Astrophysik, Garching, Germany
[3] Institutt for fysikk, NTNU, Trondheim, Norway
[4] D. V. Skobeltsyn Institute of Nuclear Physics, Moscow State University, Moscow, Russia
[5] II. Institut für Theoretische Physik, Universität Hamburg, Germany
Received 2010 September 16; accepted 2010 November 25; published 2010 December 21

ABSTRACT

High-energy photons from blazars can initiate electromagnetic pair cascades interacting with the extragalactic photon background. The charged component of such cascades is deflected and delayed by extragalactic magnetic fields (EGMFs), thereby reducing the observed point-like flux and potentially leading to multi-degree images in the GeV energy range. We calculate the fluence of 1ES 0229+200 as seen by *Fermi*-LAT for different EGMF profiles using a Monte Carlo simulation for the cascade development. The non-observation of 1ES 0229+200 by *Fermi*-LAT suggests that the EGMF fills at least 60% of space with fields stronger than $\mathcal{O}(10^{-16}$ to $10^{-15})$ G for lifetimes of TeV activity of $\mathcal{O}(10^2$ to $10^4)$ yr. Thus, the (non-)observation of GeV extensions around TeV blazars probes the EGMF in voids and puts strong constraints on the origin of EGMFs: either EGMFs were generated in a space filling manner (e.g., primordially) or EGMFs produced locally (e.g., by galaxies) have to be efficiently transported to fill a significant volume fraction as, e.g., by galactic outflows.

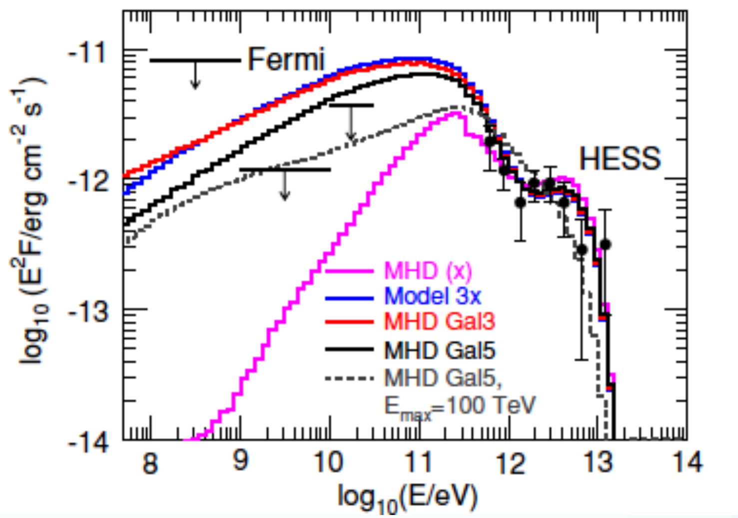

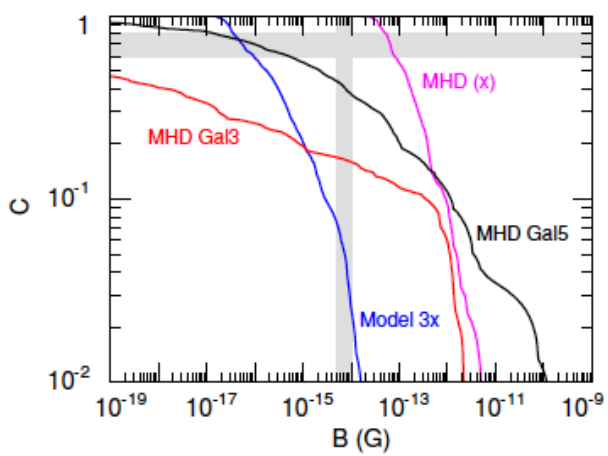

Figure 4. Cumulative volume filling factor $C(B)$ for the four different EGMF models found in MHD simulations.
(A color version of this figure is available in the online journal.)

4. SUMMARY

We have calculated the fluence of 1ES 0229+200 as seen by *Fermi*-LAT using a Monte Carlo simulation for the cascade development. We have discussed the effect of different EGMF profiles on the resulting suppression of the point-like flux seen by *Fermi*-LAT. Since the electron cooling length is much smaller than the mean free path of the TeV photons, a sufficient suppression of the point-like flux requires that the EGMF fills a large fraction along the line of sight toward 1ES 0229+200, $f \gtrsim 0.6$. The lower limit on the magnetic field strength in this volume is $B \sim \mathcal{O}(10^{-15})$ G, assuming 1ES 0229+200 is stable at least for 10^4 yr, weakening by a factor of 10 for $\tau = 10^2$ yr. These limits put very stringent constraints on the origin of EGMFs. Either the seeds for EGMFs have to be produced by a volume filling process (e.g., primordial) or very efficient transport processes have to be present which redistribute magnetic fields that were generated locally (e.g., in galaxies) into filaments and voids with a significant volume filling factor.

Primordial Magnetogenesis

F. Hoyle, in Proc.
"La structure et l'evolution de l'Universe" **(1958)**

- inflation
- phase transitions
- supersymmetry
- string cosmology
- topological defects

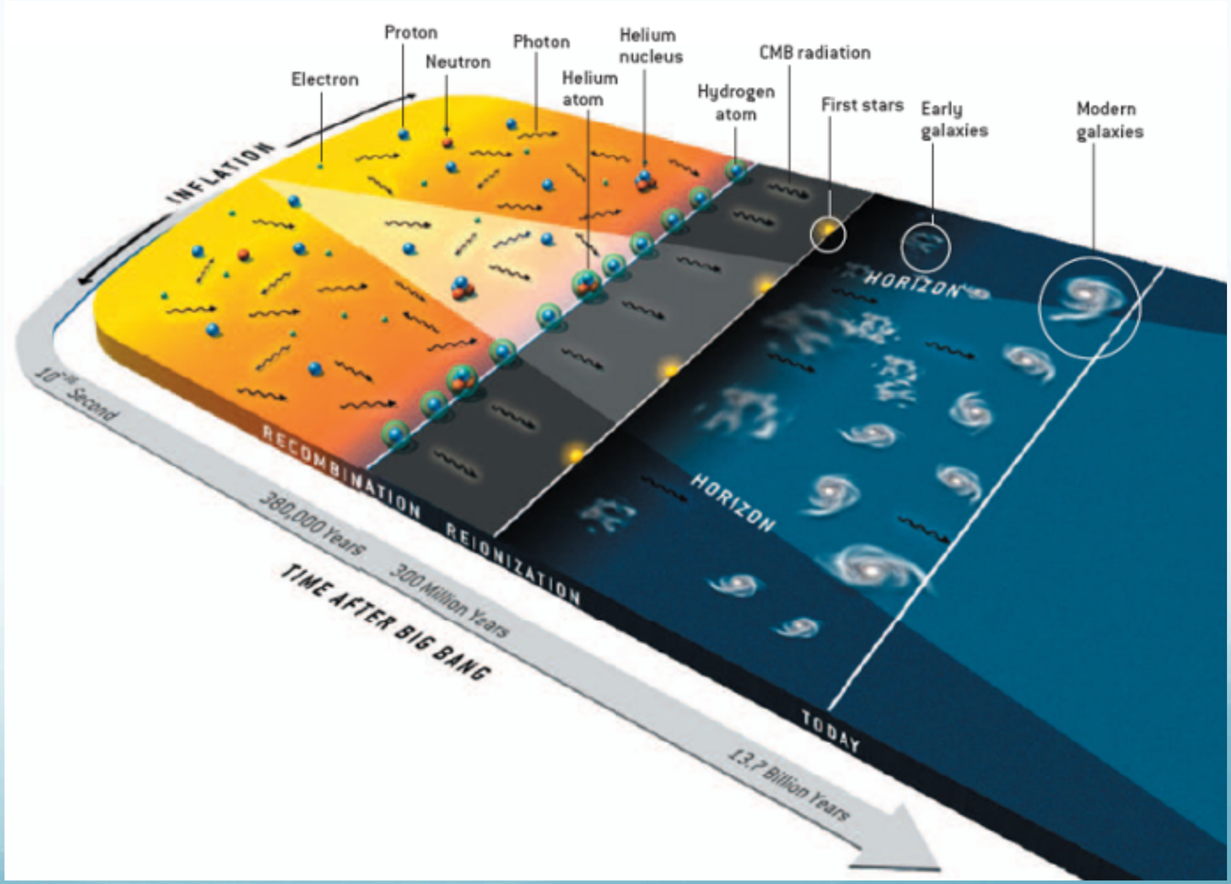

Primordial Magnetogenesis

- **Inflation**
  - the correlation length larger than horizon
  - scale invariant spectrum
  - well agree with the lower bounds
  - difficulties:
    - backreaction & symmetries violations

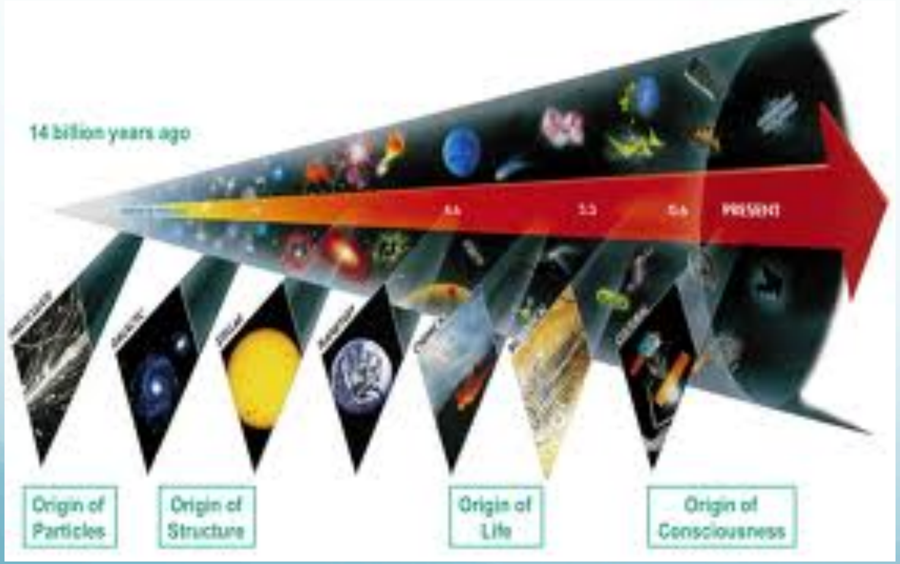

- **Phase transitions**
  - bubble collisions – first order phase transitions QCDPT or EWPT
  - causal fields
  - limited correlation length

- **chiral magnetic effect**

Testing the Early Universe

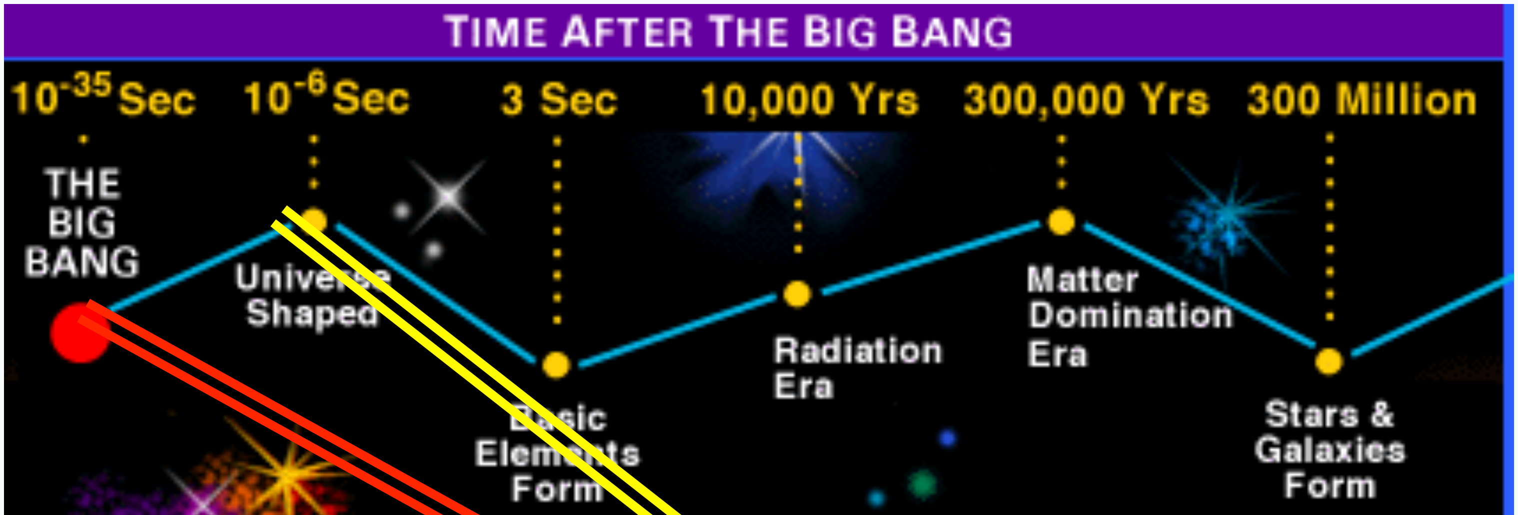

https://visav.phys.uvic.ca/~babul/AstroCourses/P303/BB-slide.htm

magnetic field origin
red-inflation
yellow- phase transitions

https://www.quantamagazine.org/the-hidden-magnetic-universe-begins-to-come-into-view-20200702/

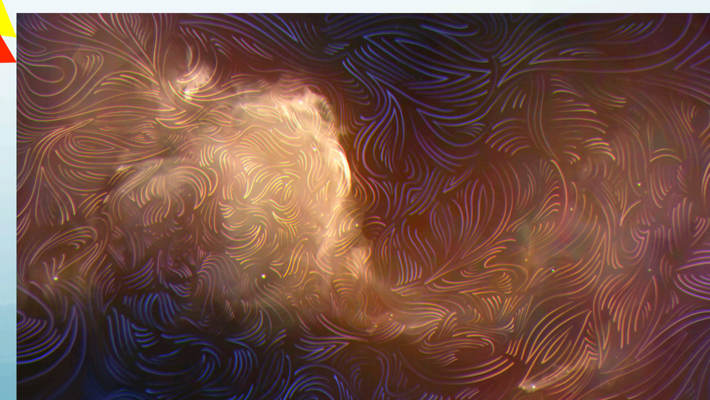

Primordial Turbulence

- primordial plasma is perfect conductor
- interaction between primordial magnetic fields and fluid (plasma)
- development of turbulence

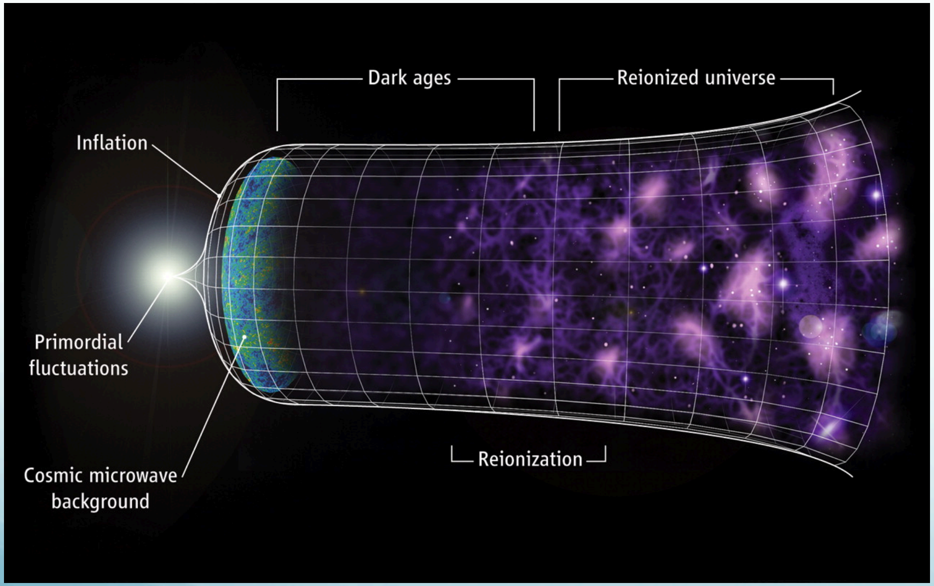

Penders, Jones, Porter, 2019

other sources of primordial turbulence?

Primordial Velocity Fields

- Cosmological Phase Transitions

Bubbles collisions and nucleation

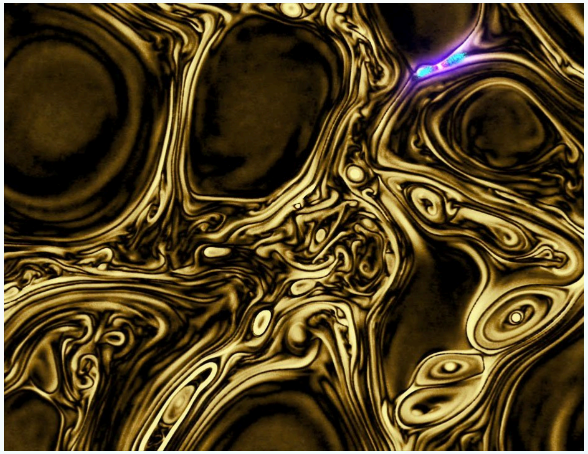

Baym et al. 1995

Quashnock, et al. 1989

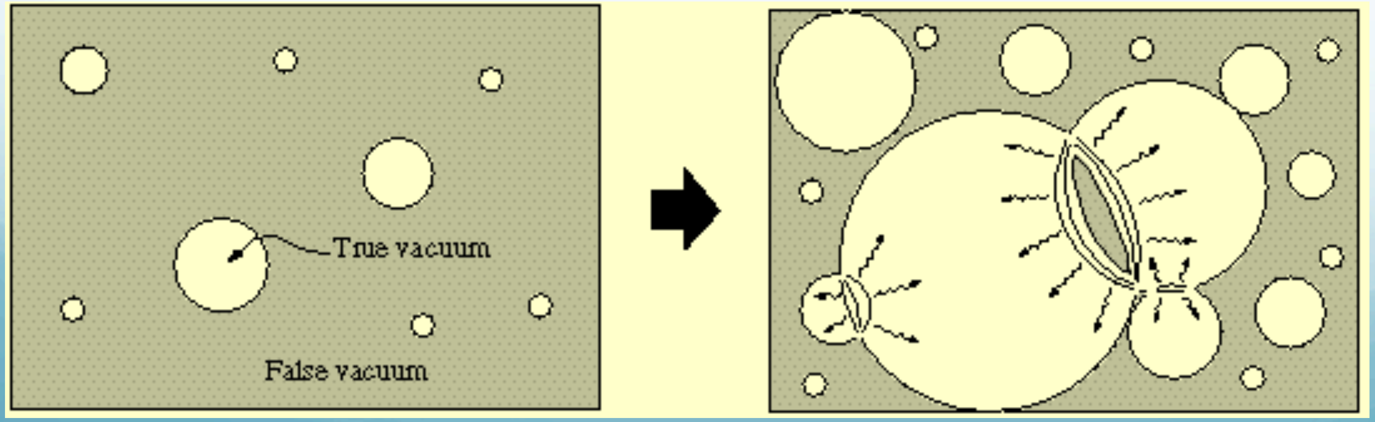

High Resolution 3D Compressible MHD Simulations - Decay

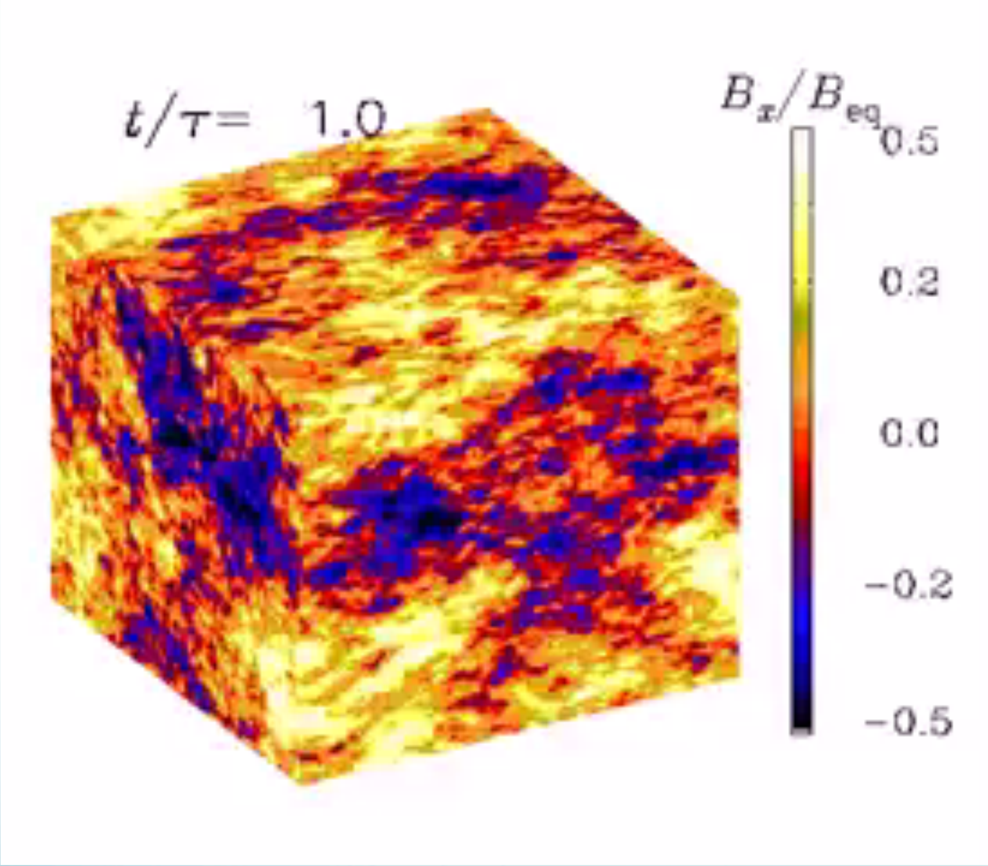

$$\frac{\partial \rho}{\partial t} + \nabla \cdot [\rho \mathbf{v}] = 0$$

$$\frac{\partial (\rho \mathbf{v})}{\partial t} + \nabla \cdot [\rho \mathbf{v}\mathbf{v} - \mathbf{B}\mathbf{B} + \mathsf{P}^*] = 0$$

$$\frac{\partial E}{\partial t} + \nabla \cdot [(E + P^*)\mathbf{v} - \mathbf{B}\,(\mathbf{B} \cdot \mathbf{v})] = 0$$

$$\frac{\partial \mathbf{B}}{\partial t} - \nabla \times (\mathbf{v} \times \mathbf{B}) = 0$$

$$P^* = P + \frac{\mathbf{B} \cdot \mathbf{B}}{2}$$

$$E = P/(\gamma - 1) + \frac{\rho(\mathbf{v} \cdot \mathbf{v})}{2} + \frac{\mathbf{B} \cdot \mathbf{B}}{2}$$

Brandenburg et al. 2015

Classes of Turbulences

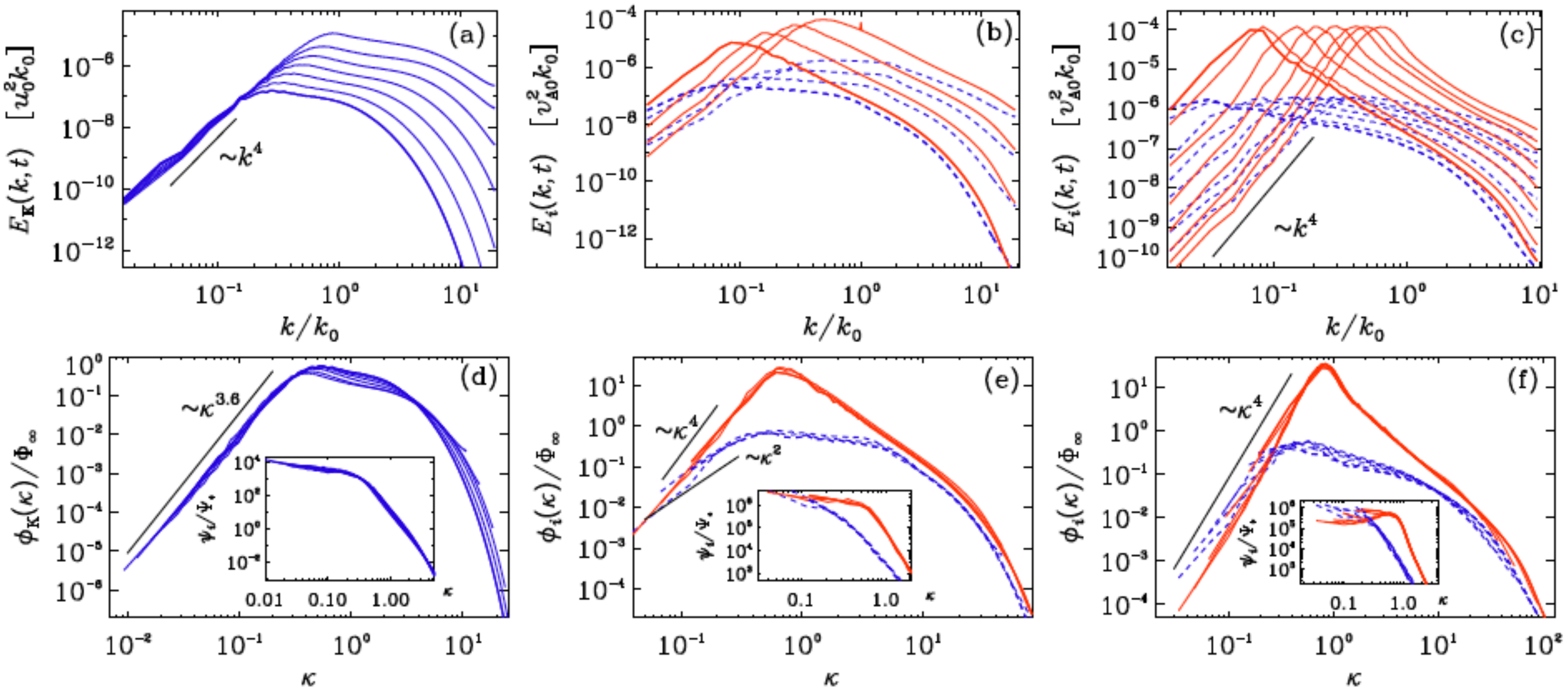

Brandenburg & Kahniashvili 2017

Classes of MHD Turbulence

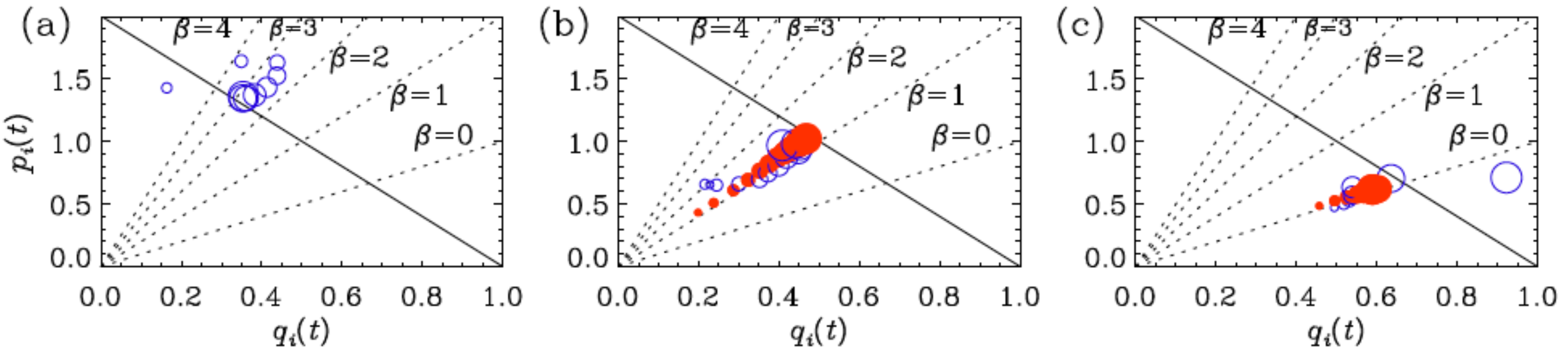

FIG. 2: pq diagrams for cases (i)–(iii). Open (closed) symbols correspond to $i=$ K (M) and their sizes increase with time.

TABLE I: Scaling exponents and relation to physical invariants and their dimensions.

β	p	q	inv.	dim.
4	$10/7 \approx 1.43$	$2/7 \approx 0.286$	$\mathcal{L}$	$[x]^7[t]^{-2}$
3	$8/6 \approx 1.33$	$2/6 \approx 0.333$		
2	$6/5 = 1.20$	$2/5 = 0.400$		
1	$4/4 = 1.00$	$2/4 = 0.500$	$\langle A_{2D}^2 \rangle$	$[x]^4[t]^{-2}$
0	$2/3 \approx 0.67$	$2/3 \approx 0.667$	$\langle A \cdot B \rangle$	$[x]^3[t]^{-2}$
-1	$0/2 = 0.00$	$2/1 = 1.000$		

$$\mathcal{E}_i(t) \sim t^{-p_i} \text{ for } i = \text{K or M}$$

$$\xi \propto t^q,$$

Brandenburg & Kahniashvili 2017

Inflationary Magnetogensis

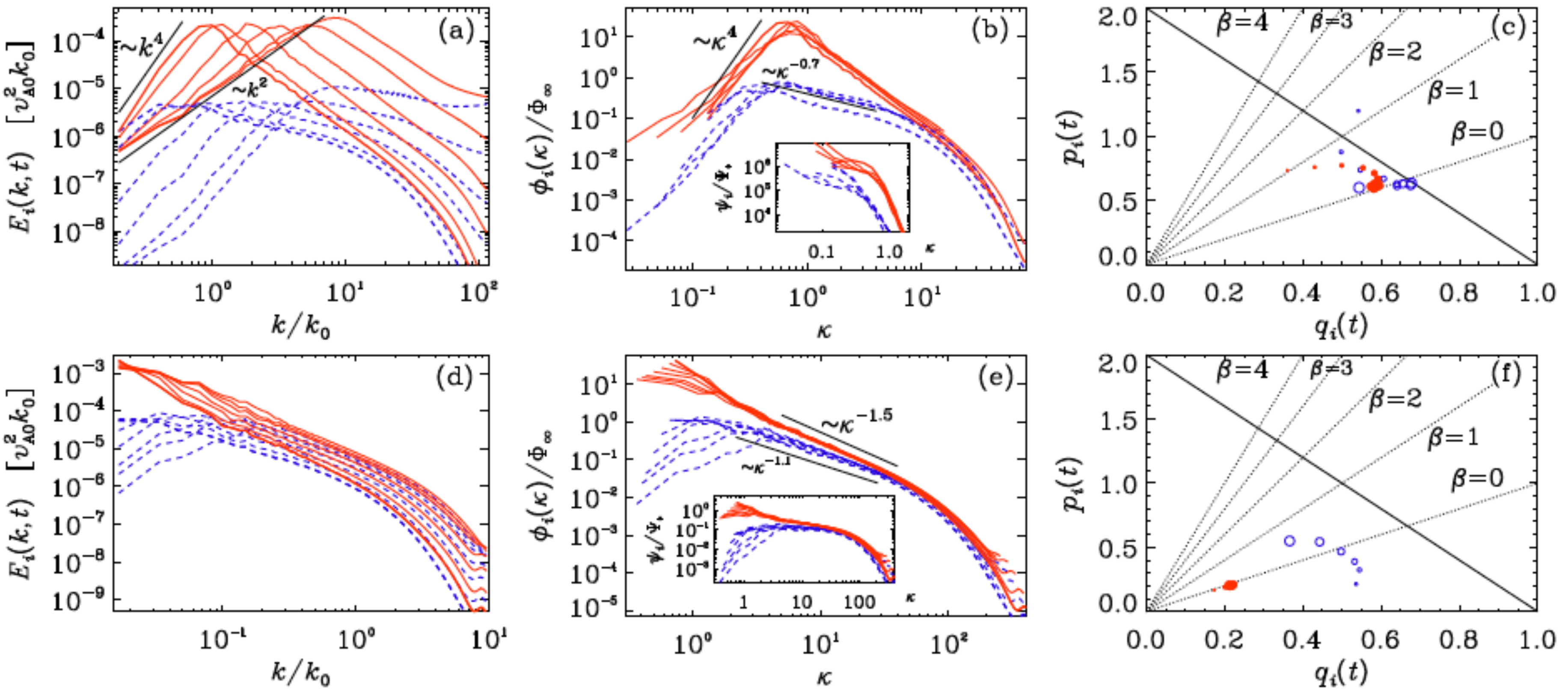

FIG. 3: E_M (solid) and E_K (dashed) in MHD with fractional helicity and $\alpha = 2$ (a), as well as full helicity and $\alpha = -1$ (d), together with compensated spectra (b,e) and the *pq* diagrams (c,f).

Brandenburg & Kahniashvili 2017

Cauchy Problem at Work - BBN

- Big Bang Nucleosynthesis
  - limits on effective number of relativistic species N_{eff}

$N_{eff}^{(\nu)} = 3.046$ *Salas & Pastor 2016*

+ CMB data $N_{eff} = 2.862 \pm 0.306$ at 95% C.L. *Fields et al. 2019*

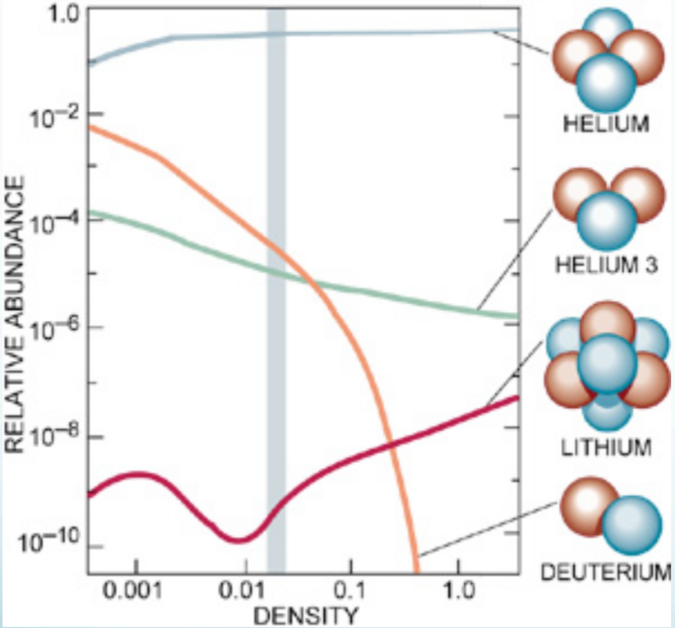

George Gamow

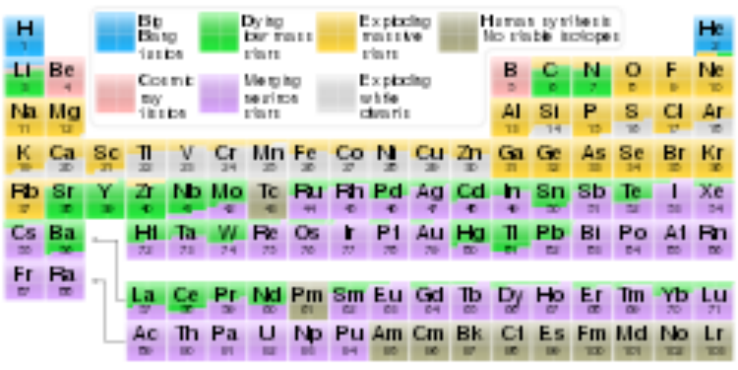

https://w.astro.berkeley.edu/~mwhite/darkmatter/bbn.html

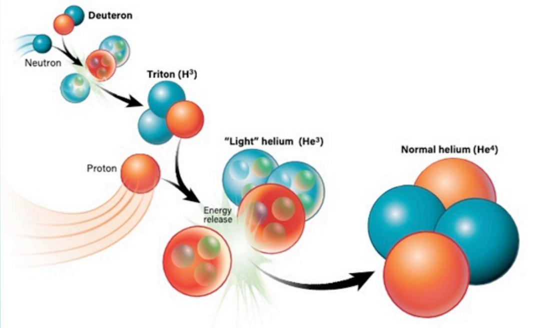

https://astronomy.com/magazine/news/2021/01/the-beginning-to-the-end-of-the-universe-the-emergence-of-matter

N_{eff}: BBN and CMB limits

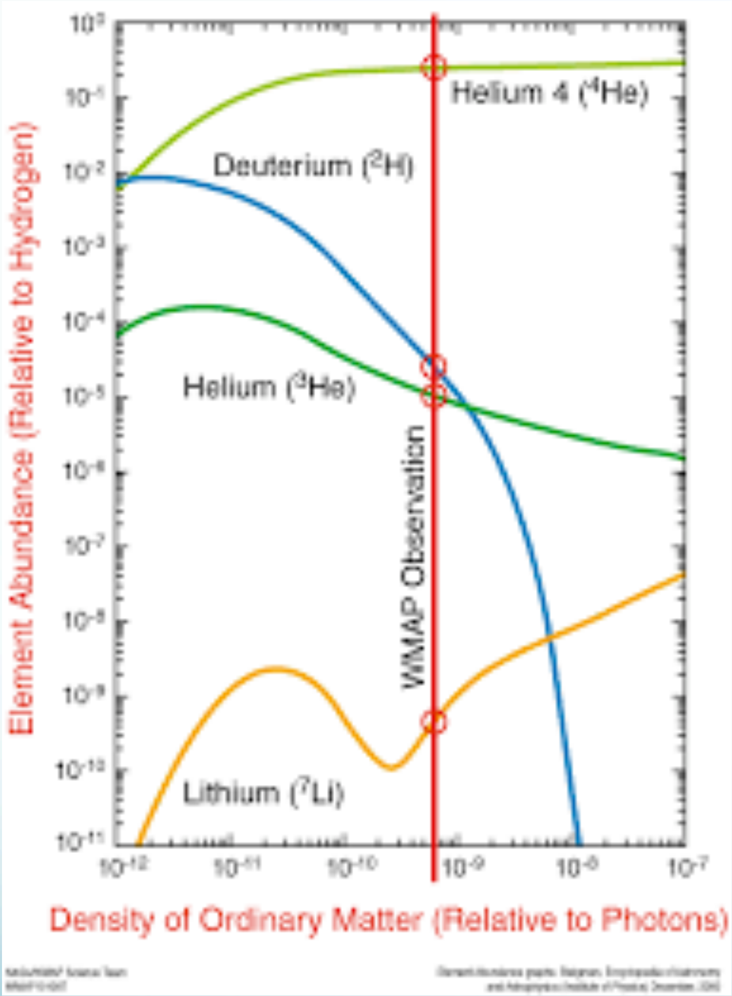

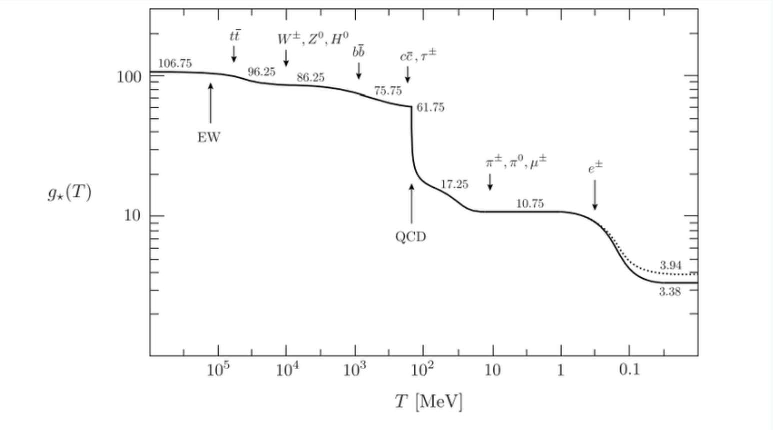

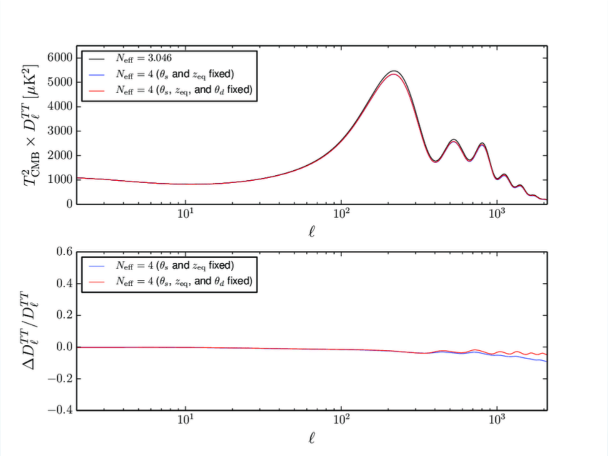

Vagnozzi 2019

https://wmap.gsfc.nasa.gov/universe/bb_tests_ele.html

N_{eff} = 2.862 ± 0.306 at 95% C.L. *Fields et al. 2019*

BBN & Primordial Magnetic Fields

- Extra radiation like energy density less than ~3% of the radiation energy density **at BBN**

$$\frac{\rho_{\rm add}}{\rho_{\rm rad}} = 0.277\left(\frac{\Delta N_{\rm eff}}{0.122}\right); \qquad \Delta N_{eff} = N_{\rm eff} - N_{\rm eff}^{\nu}$$

- The upper bound on the magnetic (effective) amplitude order of microGauss **at BBN**
- **Accounting for the magnetic field decay:**
  - **The magnetic energy density does not exceed the radiation energy density at the moment of generation**
  - **BBN bounds are satisfied**

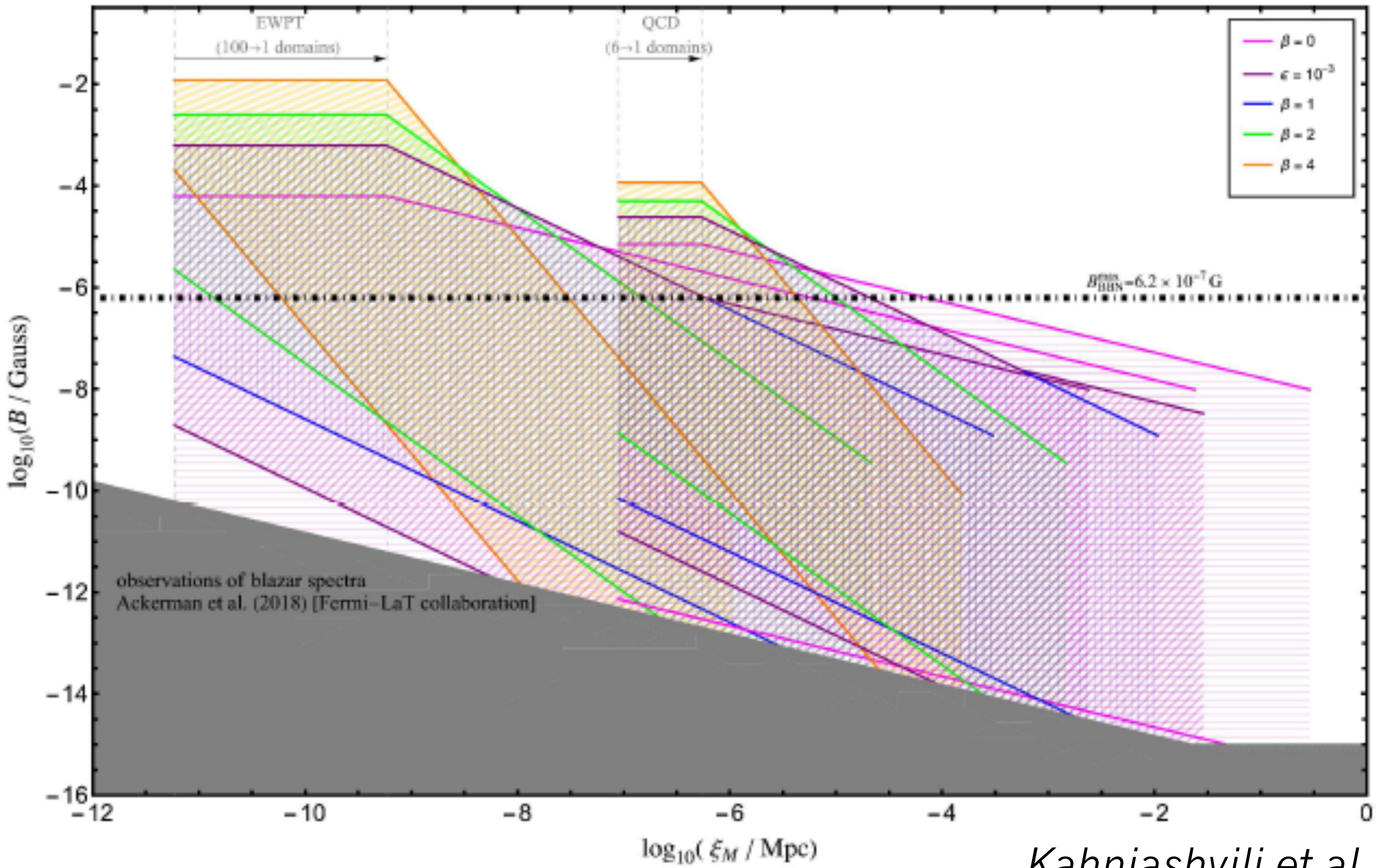

Kahniashvili et al. 2022

Possible turbulent evolution of the comoving MF strength B (and correlation length ξ_M from generation at the EW and QCD scales in the cases of fully helical ($\beta = 0$), nonhelical ($\beta = 1, 2, 4$), and partially helical MHD turbulence. Upper limits on ξ_M are determined by the size of the horizon and number of domains (bubbles) at generation, ranging from 1 to 6 (at QCD) or 100 (at EW), depending on the PT modeling. Lines terminate (on the right) at recombination (T = 0.25 eV). The upper limit of the comoving MF strength at BBN (T = 0.1 MeV) is indicated by the black dot-dashed line. Regimes excluded by observations of blazar spectra are marked in gray. The hatched regions are bounded by an (upper) limit from BBN and a (lower) limit from the blazar spectra.

Cauchy Problem at Work: CMB

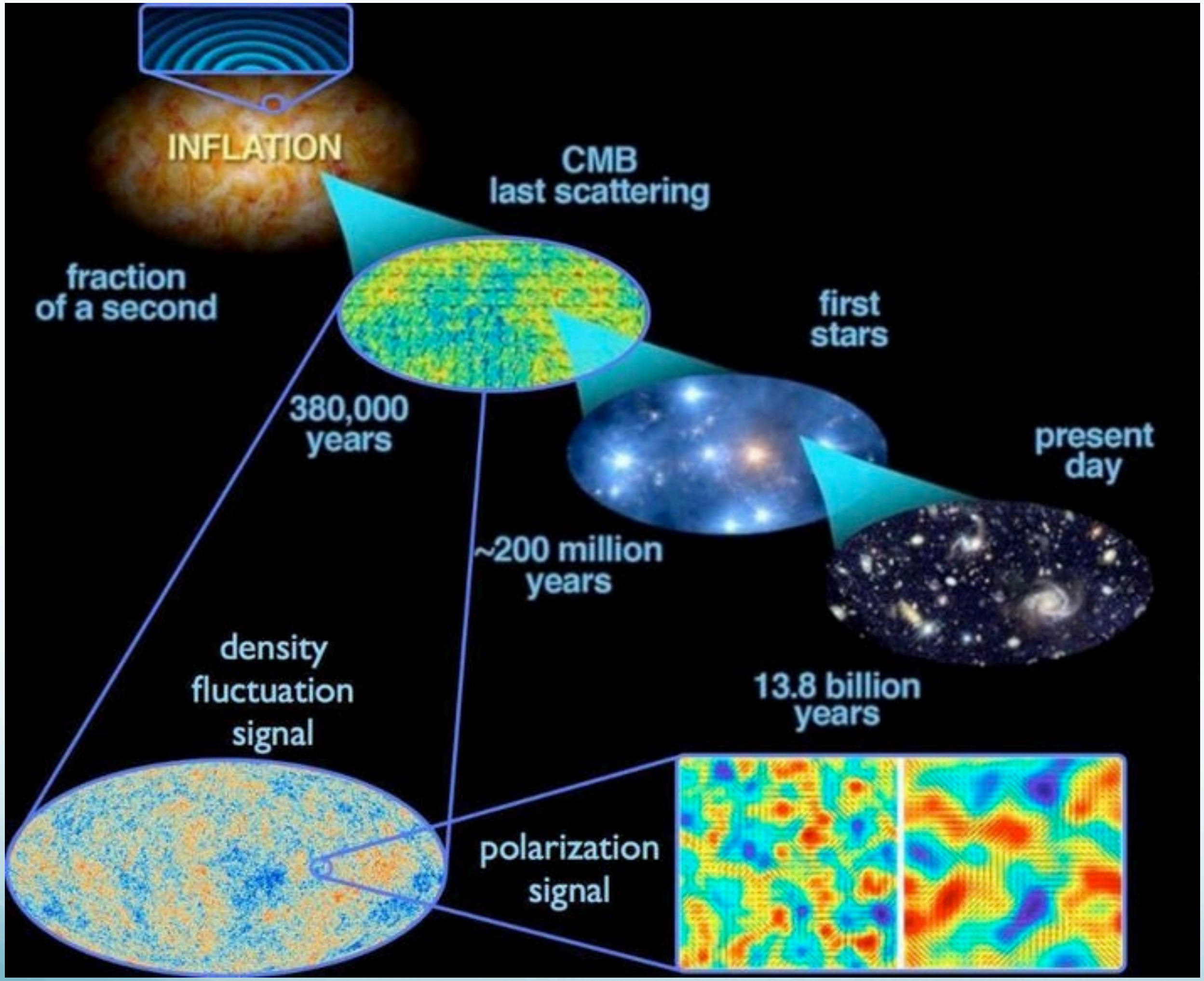

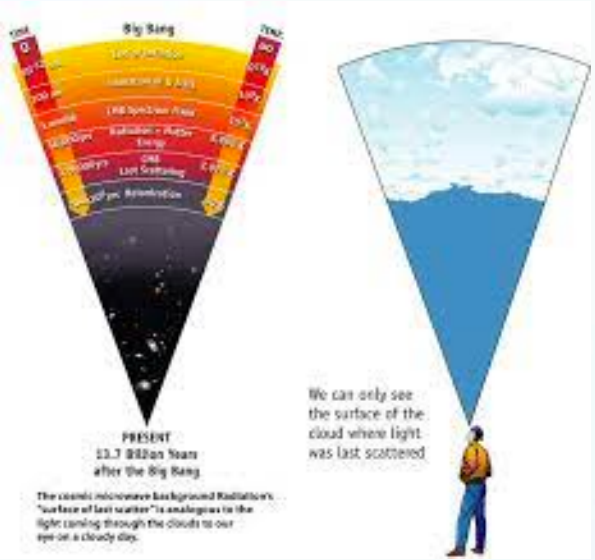

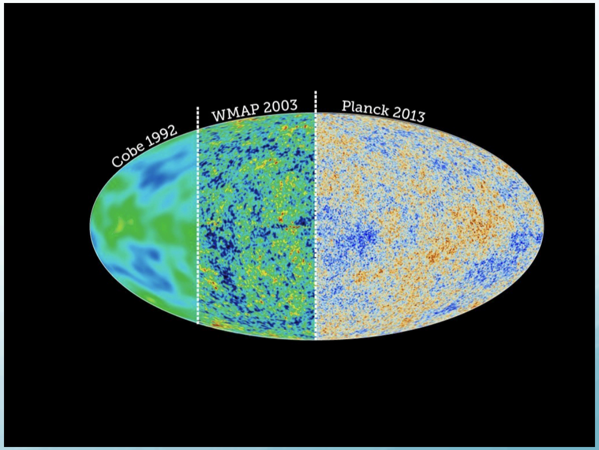

https://www.forbes.com/sites/startswithabang/2021/01/15/ask-ethan-how-does-the-cmb-reveal-the-hubble-constant/

http://abyss.uoregon.edu/~js/ast123/lectures/lec23.html

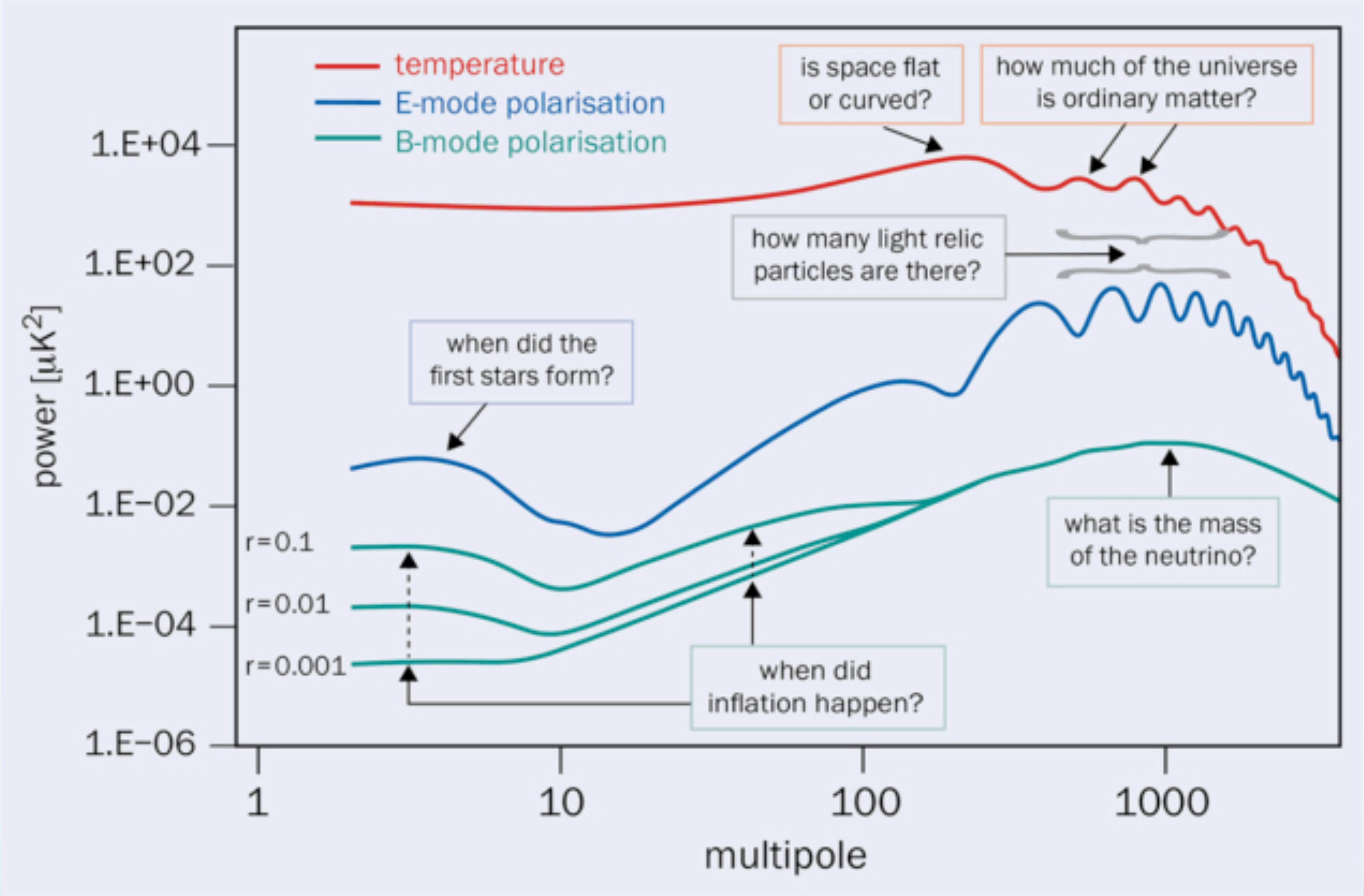

Power spectra The temperature and polarisation power spectra of the CMB, illustrating features that can answer key questions in cosmology and fundamental physics. The CMB polarisation is decomposed into a curl-free E-mode and divergence-free B-mode by analogy with electromagnetism, with r quantifying the scalar-to-tensor ratio (the size of the B-modes relative to that of the temperature power spectrum). Credit: J Borrill

https://cerncourier.com/a/exploring-the-cmb-like-never-before/

Primordial Magnetic Fields & CMB

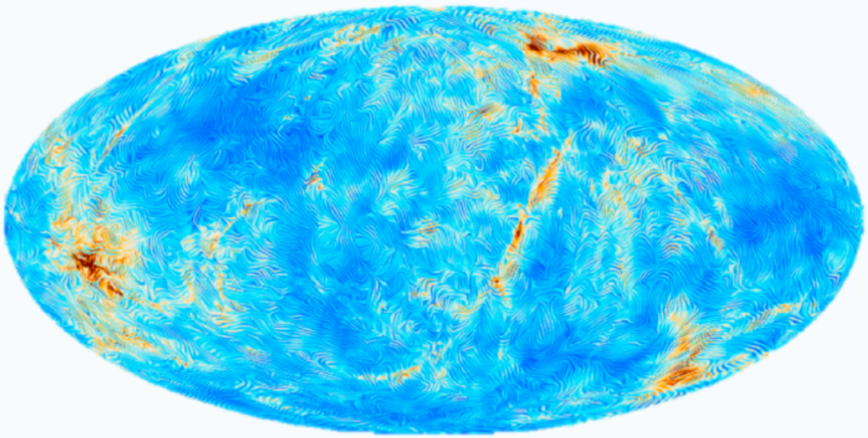

Harrison PMFs on a 60 Mpc distance today, *Hutschenreuter et al. 2018*

INAF OAS BOLOGNA

Looking for the origin of cosmic magnetism

by Daniela Paoletti

Gravitational perturbations ➘

Magnetic Fields or Turbulent source ➘

$$G_{ik} = 8\pi G T_{ik}$$

Planck 2015 results. XIX: Constraints on primordial magnetic fields

- **density perturbations -** scalar mode
  - Fast and slow magnetosound waves
- **vorticity perturbations** - vector mode
  - Alfven waves
- **gravitational waves** – tensor mode

CMB Imprints

- Polarization B-mode
  - Additional source from the vector (vortical) and tensor (gravitational waves) modes
  - Parity-odd cross correlations
  - Faraday rotation

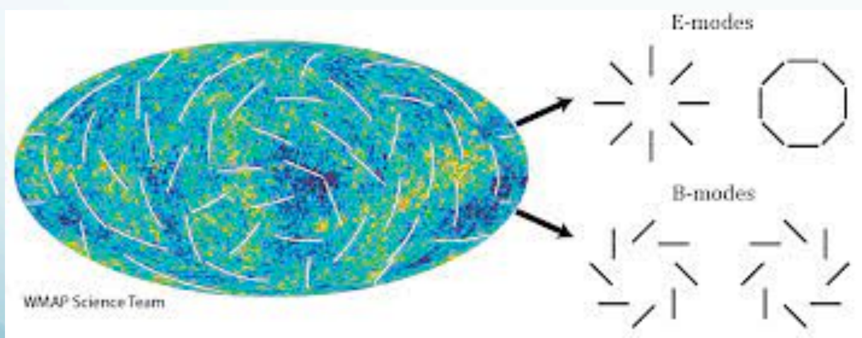

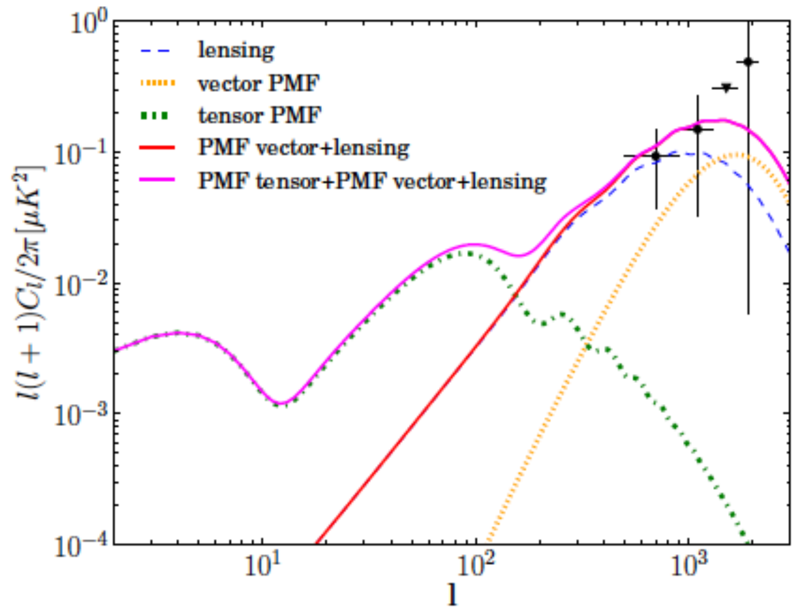

FIG. 4: A representative B-mode polarization power spectrum sourced by a scale-invariant PMF. Shown are the passive tensor mode (green), the compensated vector mode (orange), the gravitational lensing contribution (blue) and the combinations of the lensing and vector B modes (red) and all three components (magenta). The PMF contribution is based on $B_{1\mathrm{Mpc}} = 2.5$ nG, $n = -2.9$, $a_\nu/a_{\mathrm{PMF}} = 10^9$. The data points are from the POLARBEAR first-season B-mode power spectrum. The third point is the 95% upper limit assuming the band power is positive.

POLARBEAR 2015

CMB Challenges: Foregrounds

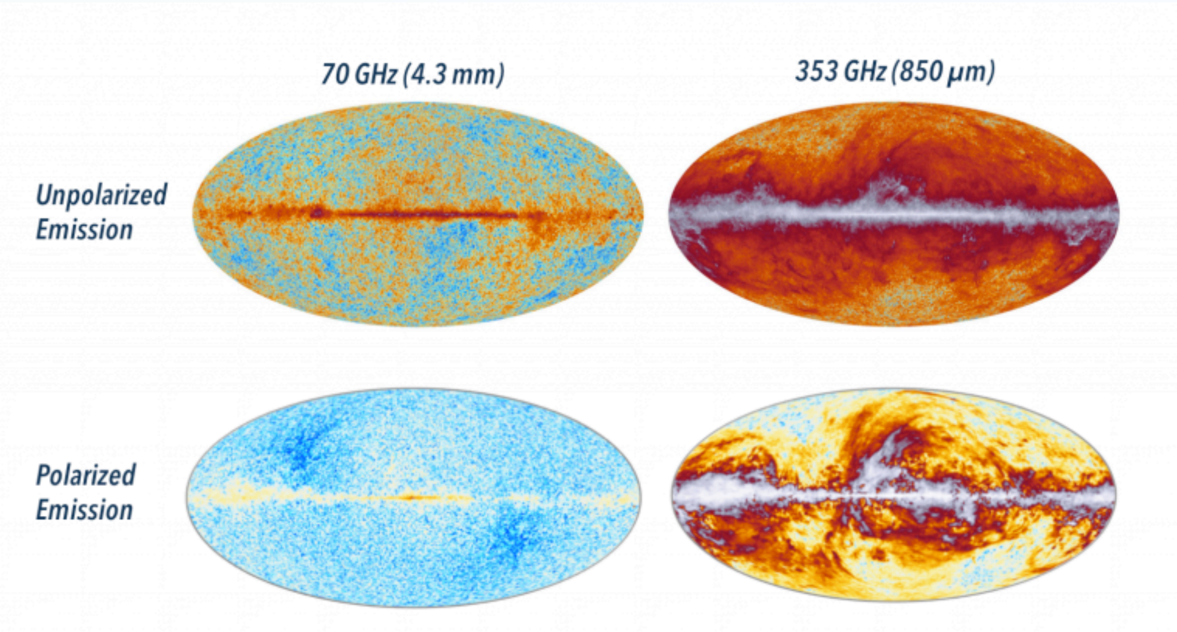

https://sites.northwestern.edu/blast/diffuse-ism-cmb-foregrounds/

Maps of the intensity of polarized and unpolarized galactic emission at CMB millimeter wavelengths (left) and submillimeter wavelengths (right).

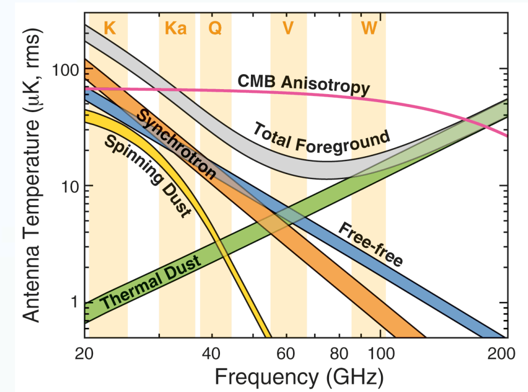

Bennett et al. 2013

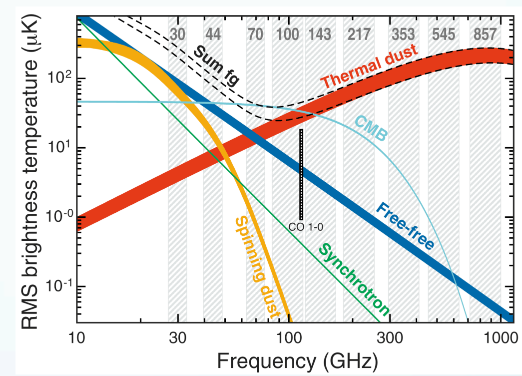

Planck 2015 Results X

Lambda Data Products

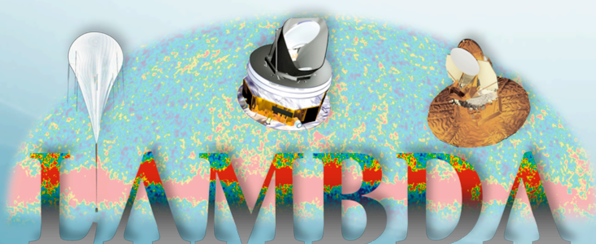

https://lambda.gsfc.nasa.gov/product/foreground/

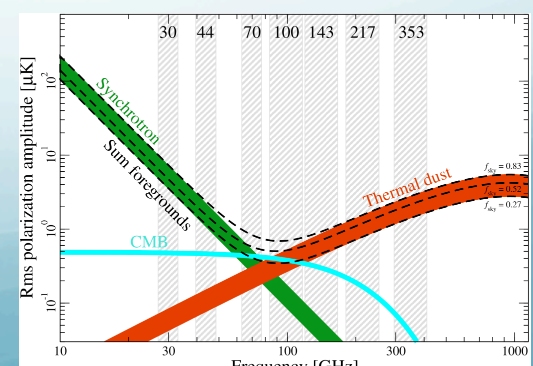

Planck 2018 Results IV

Cauchy Problem at Work: Gravitational Waves

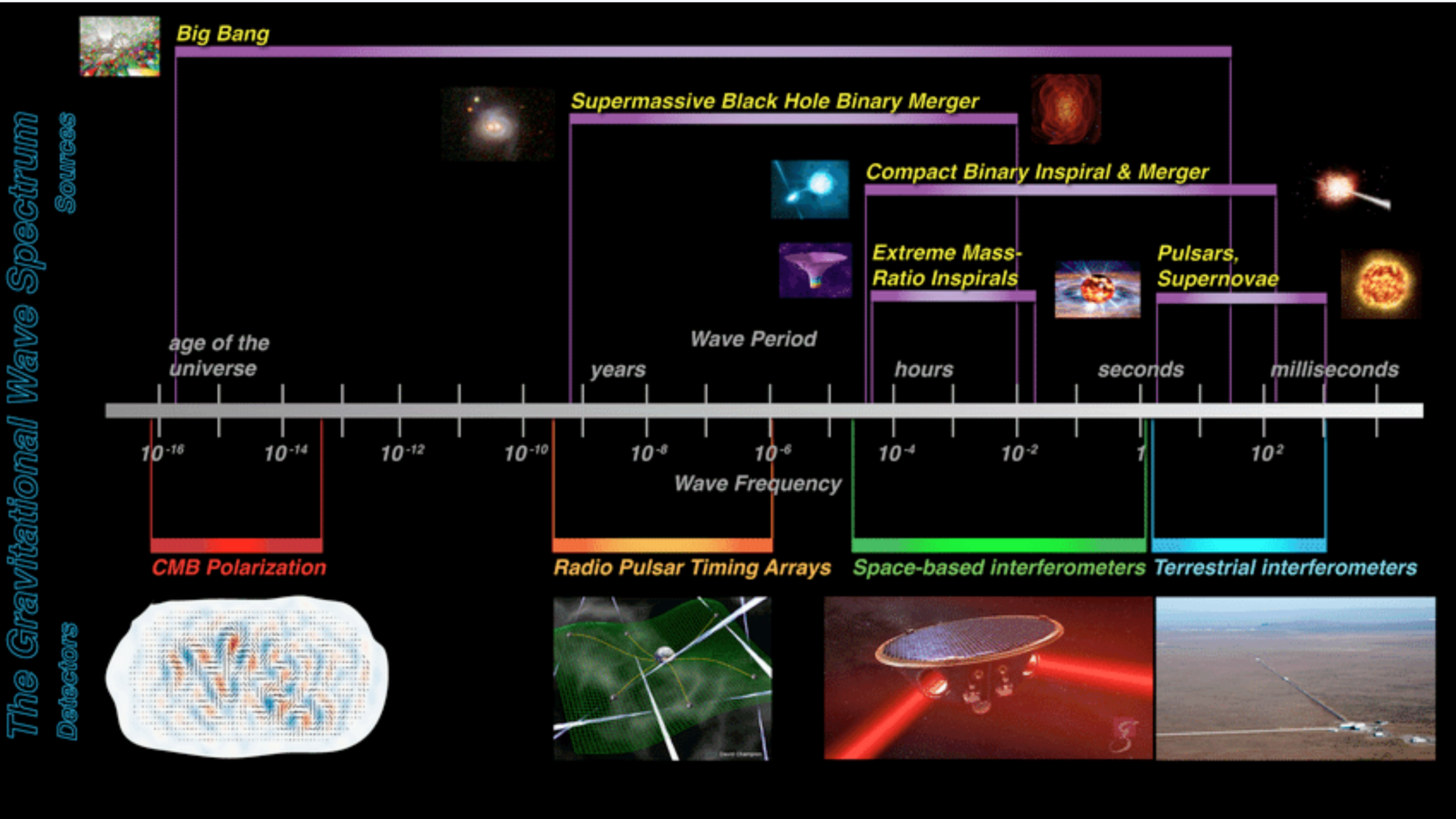

Living Rev Relativ (2017) 20:2
https://doi.org/10.1007/s41114-017-0004-1

CrossMark

REVIEW ARTICLE

Detection methods for stochastic gravitational-wave backgrounds: a unified treatment

Joseph D. Romano[1] · Neil. J. Cornish[2]

A cosmological background produced by the superposition of a large number of independent gravitational-wave signals from the early Universe is expected to be Gaussian (via the central limit theorem), as well as isotropically-distributed on the sky. Contrast this with the superposition of gravitational waves produced by unresolved Galactic white-dwarf binaries radiating in the LISA band (10^{-4} Hz to 10^{-1} Hz). Although this confusion-limited astrophysical foreground is also expected to be Gaussian and stationary, it will have an anisotropic distribution, following the spatial distribution of the Milky Way. The anistropy will be encoded as amodulation in the LISA output, due to the changing antenna pattern of the LISA constellation in its yearly orbit around the Sun.

Removing Foregrounds

Measuring the primordial gravitational-wave background in the presence of astrophysical foregrounds

Sylvia Biscoveanu,[1, 2, 3, a] Colm Talbot,[4, 2, 3] Eric Thrane,[2, 3] and Rory Smith[2, 3]

[1]*LIGO, Massachusetts Institute of Technology, Cambridge, Massachusetts 02139, USA*
[2]*School of Physics and Astronomy, Monash University, VIC 3800, Australia*
[3]*OzGrav: The ARC Centre of Excellence for Gravitational-Wave Discovery, Clayton, VIC 3800, Australia*
[4]*LIGO, California Institute of Technology, Pasadena, CA 91125, USA*

Primordial gravitational waves are expected to create a stochastic background encoding information about the early Universe that may not be accessible by other means. However, the primordial background is obscured by an astrophysical foreground, consisting of gravitational waves from compact binaries. We demonstrate a Bayesian method for estimating the primordial background in the presence of an astrophysical foreground. Since the background and foreground signal parameters are estimated simultaneously, there is no subtraction step, and therefore we avoid astrophysical contamination of the primordial measurement, sometimes referred to as "residuals." Additionally, since we include the non-Gaussianity of the astrophysical foreground in our model, this method represents the statistically optimal approach to the simultaneous detection of a multi-component stochastic background.

Phys. Rev. Lett. 125, 241101 (2020)

Primordial Magnetic Fields and Gravitational Waves

Mon. Not. R. astr. Soc. (1987) **229**, 357–370

$$\nabla^2 h_{ij}(\boldsymbol{x},t) - \frac{\partial^2}{\partial t^2} h_{ij}(\boldsymbol{x},t) = -16\pi G\, S_{ij}(\boldsymbol{x},t)$$

Generation of gravitational waves by the anisotropic phases in the early Universe

D. V. Deryagin, D. Yu. Grigoriev and
V. A. Rubakov *Institute for Nuclear Research, USSR Academy of Sciences, Moscow 117312, USSR*
M. V. Sazhin *P. K. Sternberg Astronomical Institute, Universitetskii pr. 13, Moscow 119899, USSR*

The space interferometer will be a unique device to observe the gravitational radiation from anisotropic phases possible at the energy scales 1TeV-100GeV.

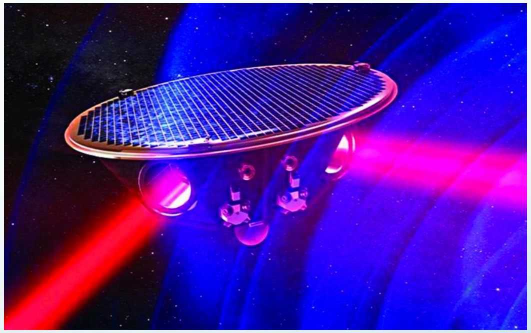

Pulsar Timing Array (PTA) are sensible to gravitational waves generated or present at QCD energy scales

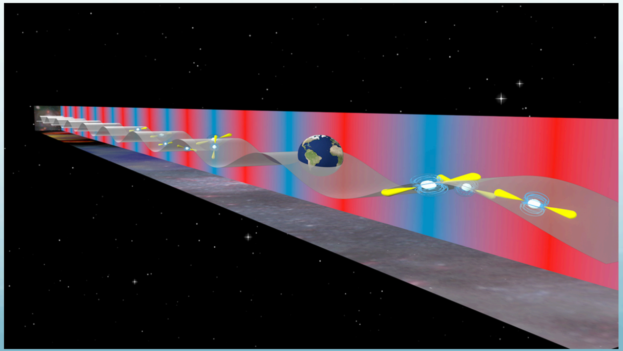

Gravitational Waves from Turbulence

$$\nabla\, \delta\rho\,(\mathbf{x},t) - \frac{1}{c_s^2}\frac{\partial^2}{\partial t^2}\,\delta\rho\,(\mathbf{x},t) = -\frac{\partial^2}{\partial x^i \partial x^j}\; T_{ij}\,(\mathbf{x},t), \qquad c_s^2 = \frac{\partial p}{\partial \rho}$$

$$\nabla^2 h_{ij}(\boldsymbol{x},t) - \frac{\partial^2}{\partial t^2} h_{ij}(\boldsymbol{x},t) = -16\pi G\, S_{ij}(\boldsymbol{x},t)$$

$$c = 1$$

Aero-acoustic approximation:

- ✓ sound waves generation by turbulence
- ✓ gravitational waves generation

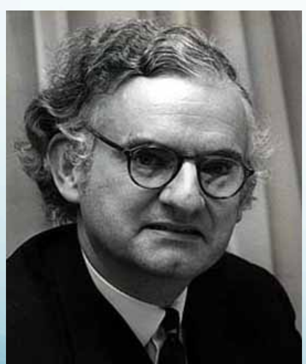

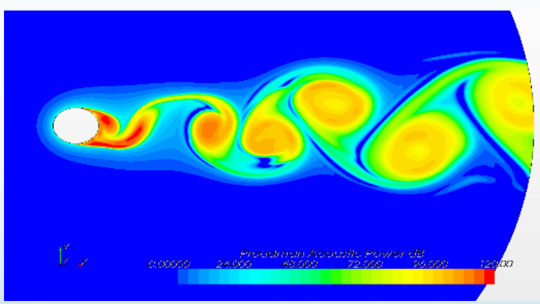

Lighthill, 1952; Proudman 1952

Kosowsky, Mack, Kahniashvili, 2002
Dolgov, Grasso, Nicolis, 2002

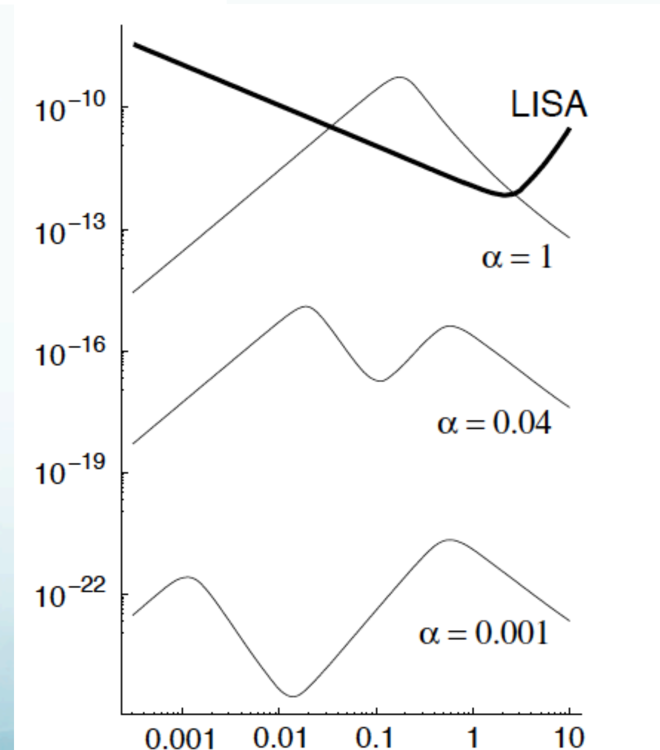

Nicolis 2004

Numerical Simulations

- To account properly non-linear processes (MHD)
- Not be limited by the short duration of the phase transitions
- Two stages turbulence decay
  - Forced turbulence
  - Free decay
- The source is present till recombination (after the field is frozen in)
- Results – strongly initial conditions dependent

Roper Pol et al. 2019

$$\left(\frac{\partial^2}{\partial t^2} - c^2\nabla^2\right) h_{ij}^{\mathrm{TT}} = \frac{16\pi G}{a^3c^2} T_{ij}^{\mathrm{TT}},$$

Grishchuk 1974 $h_{ij}^{\mathrm{TT}} = a h_{ij}^{\mathrm{TT,phys}}$

$$\mathrm{d}t_{\mathrm{phys}} = a\mathrm{d}t$$

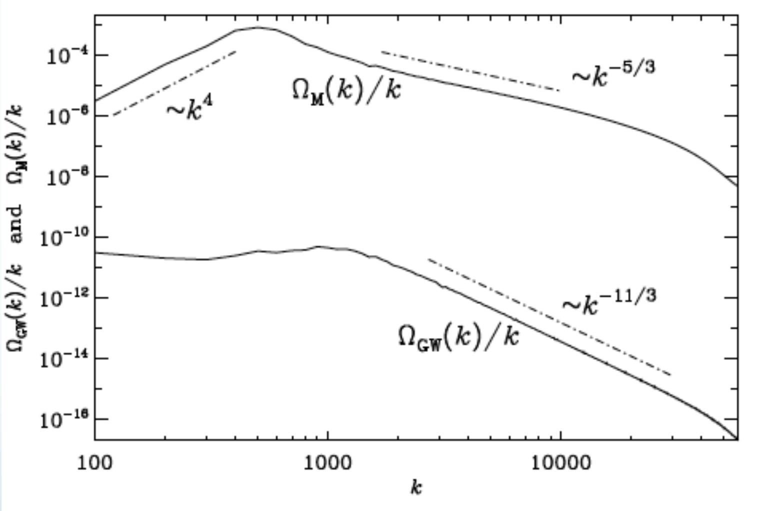

Magnetic and GW energy spectra averaged over late times (t > 1.1), after the GW spectrum has started to fluctuate around a steady state.

Why Numerical Modeling Is Necessary

- ✓ It is assumed the stationary turbulence while in reality turbulence decays

$$\mathcal{E}_M(t) \simeq \mathrm{w} b_1^2 \left(1 + \frac{t}{\tau_1}\right)^{-2/3},$$

$$\mathcal{E}_v(t) \simeq \mathrm{w} v_1^2 \left(1 + \frac{t}{\tau_1}\right)^{-2/3},$$

- ✓ Three stages of generation

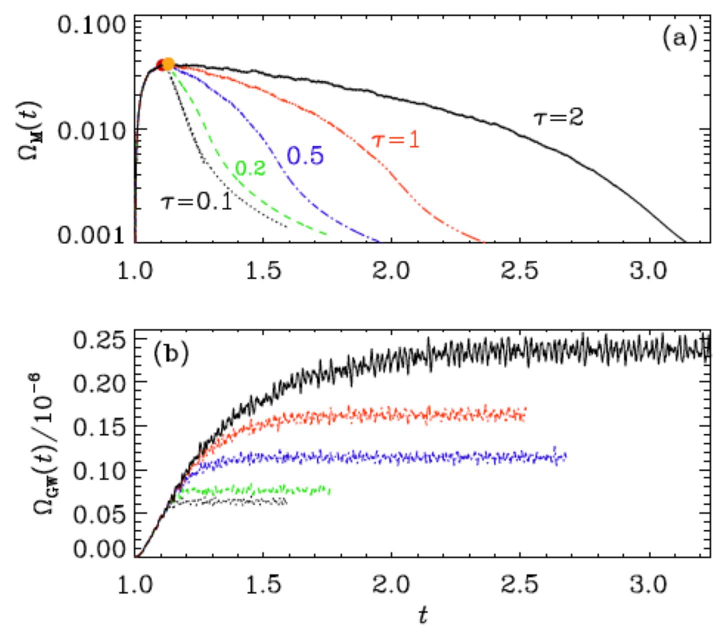

FIG. 1: Evolution of magnetic energy (top) and growth of GW energy density (bottom) for simulations where the driving is turned off at $t = 1.1$ (black dotted line), or the strength of the driving is reduced linearly in time over the duration $\tau = 0.2$ (green), 0.5 (blue), 1 (red), or 2 (black). Time is in units of the Hubble time at the moment of source activation.

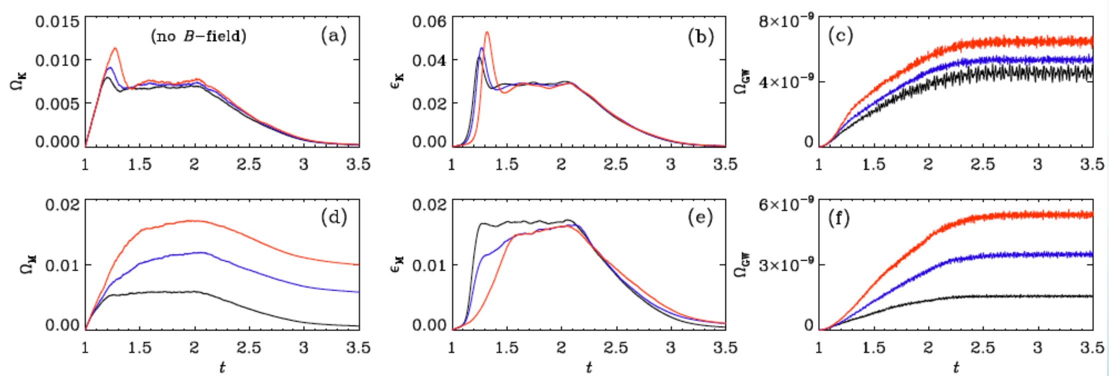

FIG. 2: Evolution of (a) Ω_K, (b) ϵ_K, and (c) Ω_{GW} for kinetically driven cases with $\sigma = 0$ (black), 0.5 (blue), and 1 (red), and of (d) Ω_M, (e) ϵ_M, and (f) Ω_{GW} for magnetically driven cases with $\sigma = 0$ (black), 0.3 (blue), and 1 (red).

Kahniashvili et al. 2020

Polarization Spectra

Assuming *stationary Kolmogoroff like turbulence* or *stationary helical Kolmogoroff turbulence*

$$\mathcal{P}(k) = \frac{\langle h_+^\star(\mathbf{k})h_+(\mathbf{k}') - h_-^\star(\mathbf{k})h_-(\mathbf{k}')\rangle}{\langle h_+^\star(\mathbf{k})h_+(\mathbf{k}') + h_-^\star(\mathbf{k})h_-(\mathbf{k}')\rangle} = \frac{\mathcal{H}(k)}{H(k)}.$$

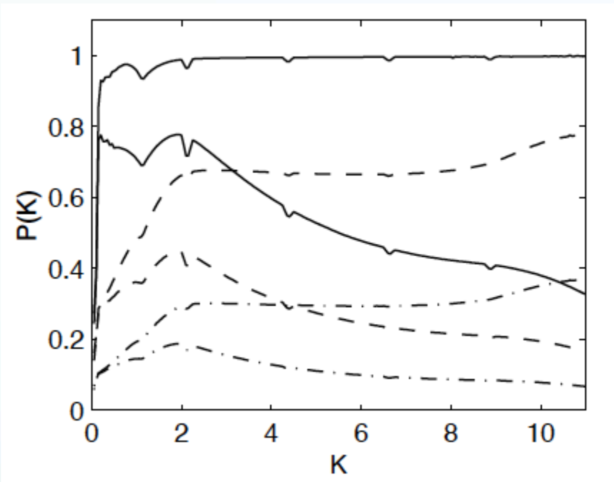

Kahniashvili et al, 2005

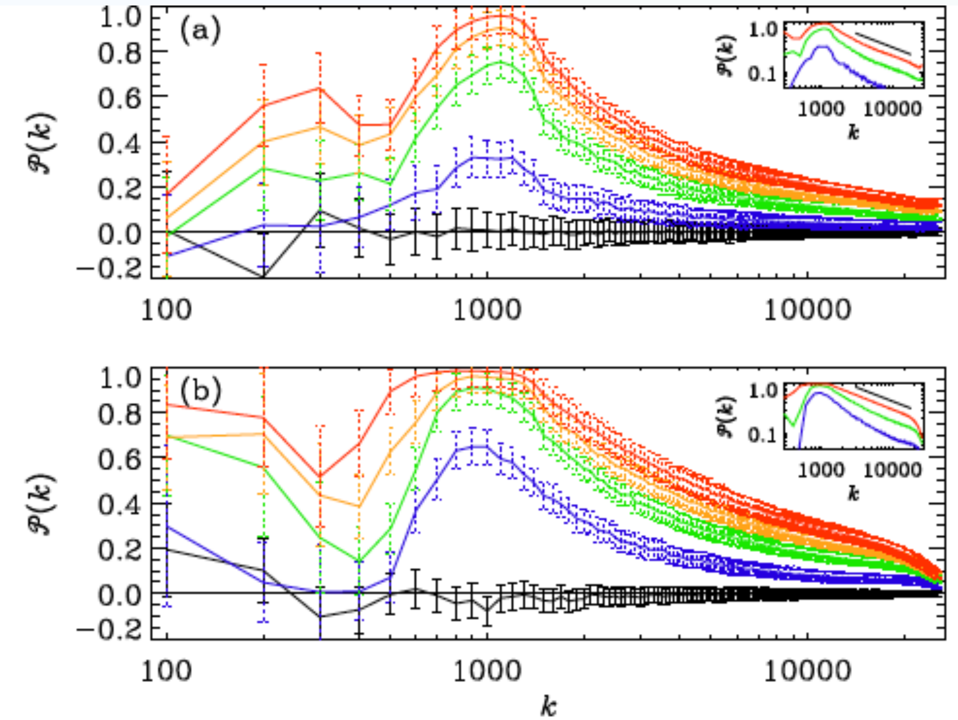

FIG. 3: Degree of circular polarization for (a) kinetically and (b) magnetically forced cases with $\sigma = 0$ (black) 0.1 (blue), 0.3 (green), 0.5 (orange), and 1 (red). Approximate error bars based on the temporal fluctuations and statistical spread for different random seeds of the forcing are shown as solid black lines for $\sigma = 0$ and as dotted lines otherwise.

Polarization spectrum retains information on parity violation at large wavelengths

- **Inverse cascading?**

Kahniashvili et al. 2020

Detection Prospects

Measuring the net circular polarization of the stochastic gravitational wave background with interferometers

Valerie Domcke [a], Juan García-Bellido [b], Marco Peloso [c,d], Mauro Pieroni [b,e], Angelo Ricciardone [c], Lorenzo Sorbo [f], Gianmassimo Tasinato [g]

Abstract

Parity violating interactions in the early Universe can source a stochastic gravitational wave background (SGWB) with a net circular polarization. In this paper, we study possible ways to search for circular polarization of the SGWB with interferometers. Planar detectors are unable to measure the net circular polarization of an isotropic SGWB. We discuss the possibility of using the dipolar anisotropy kinematically induced by the motion of the solar system with respect to the cosmic reference frame to measure the net circular polarization of the SGWB with planar detectors. We apply this approach to LISA, re-assessing previous analyses by means of a more detailed computation and using the most recent instrument specifications, and to the Einstein Telescope (ET), estimating for the first time its sensitivity to circular polarization. We find that both LISA and ET, despite operating at different frequencies, could detect net circular polarization with a signal-to-noise ratio of order one in a SGWB with amplitude $h^2\Omega_{\rm GW} \simeq 10^{-11}$. We also investigate the case of a network of ground based detectors. We present fully analytical, covariant formulas for the detector overlap functions in the presence of circular polarization. Our formulas do not rely on particular choices of reference frame, and can be applied to interferometers with arbitrary angles among their arms.

- ✓ Dipolar anisotropy introduced by our proper motion, *Seto 2006* (for LISA and ET)
- ✓ Curvature of the Earth for ground based detectors, Seto & Taruya 2007, 2008

Domske et al. 2019:
In the present work we reconsider previous results by taking into account the full response functions and noise curves in the entire frequency band (for planar detectors). Moreover, we provide fully analytical and covariant expressions for the (parity-sensitive) response functions of a ground-based detector network.

Pulsar Timing Arrays: nanoGrav

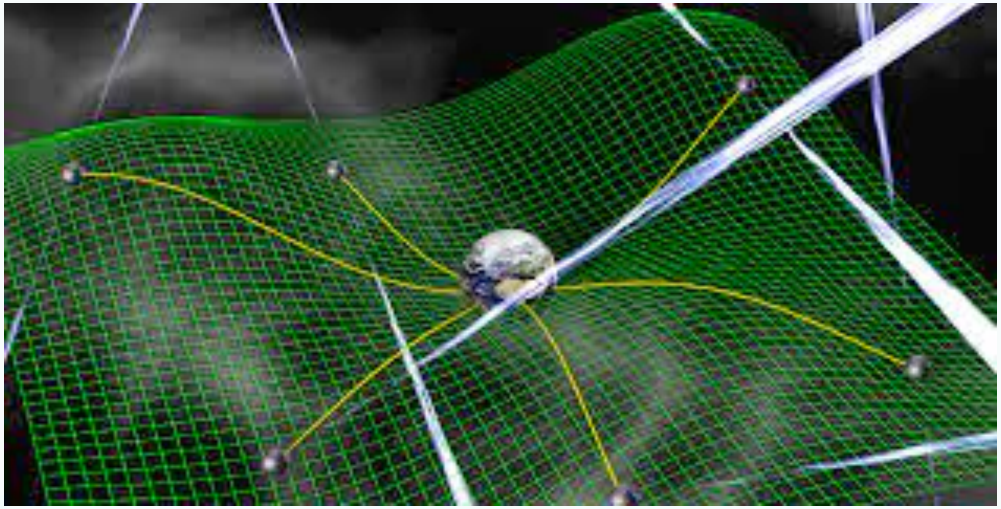

$$h_c(f) = A_{\rm CP}\left(\frac{f}{f_{\rm yr}}\right)^{\alpha_{\rm CP}},$$

$$\Omega_{\rm GW}(t,f) = \frac{1}{\mathcal{E}_{\rm crit}(t)}\frac{d\mathcal{E}_{\rm GW}}{d\ln f}$$

NANOGrav 12.5-year sensitivity range of 1–100 nHz

$$\Omega_{\rm GW}(f) = \frac{2\pi^2}{3H_0^2}f^2h_c^2(f) = \Omega_{\rm GW}^{\rm yr}\left(\frac{f}{f_{\rm yr}}\right)^{5-\gamma_{\rm CP}}$$

Arzoumanian et al (2021)

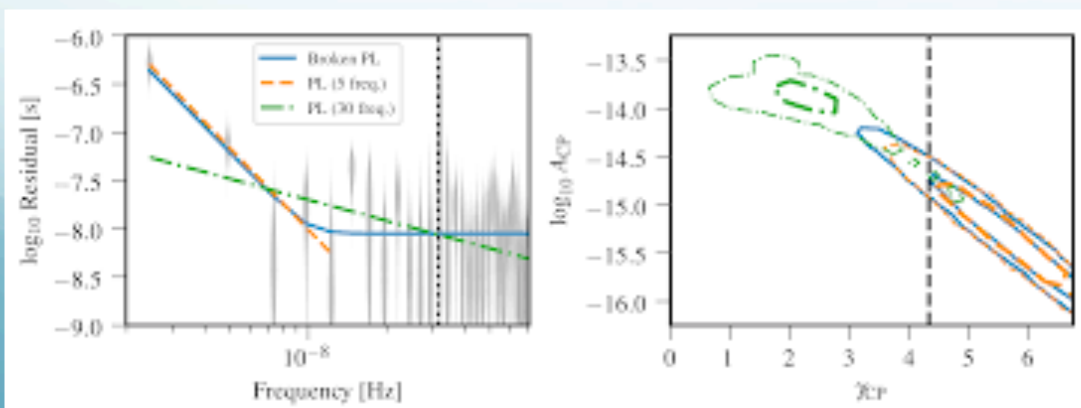

Astrophysical:
✓ Super massive black hole binary (SMBI
(Phinney 2001): γ=13/3

Cosmological:
✓ Bubbles collisions (Kosowsky et. Al. 19
✓ Inflation (Vagnozzi 2020)
✓ Cosmic strings (Blanco-Pillado et al. 2020)
✓ Seed magnetic fields and MHD Turbulence (Neronov et. al. 2020)
✓ Hydrodynamic and MHD Turbulence (Brandenburg et al. 2021)

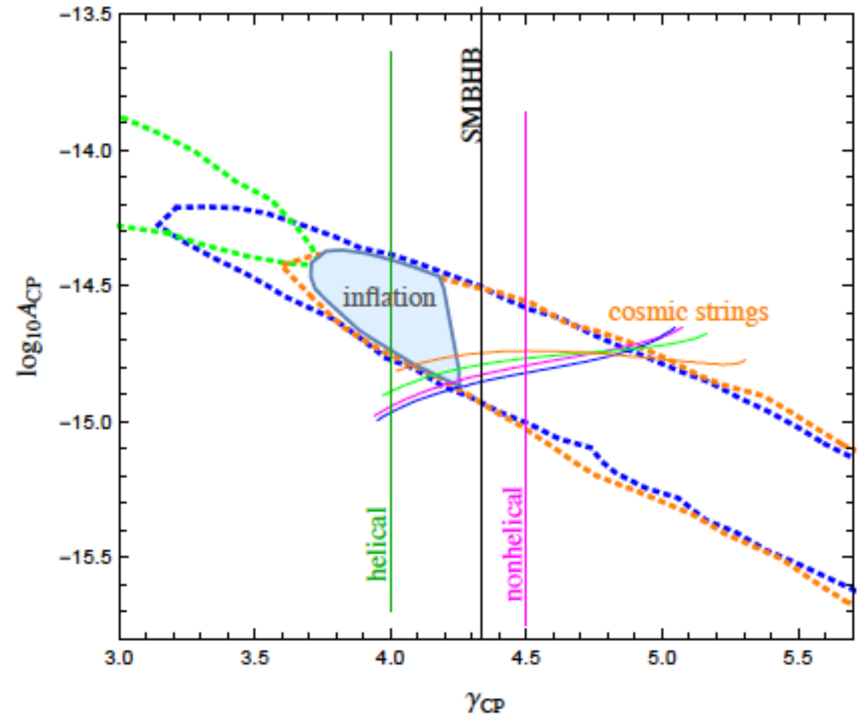

Credit: Emma Clarke

QCD energy scale

$$\frac{a_0}{a_\star} = 10^{12}\left(\frac{g_{S,\star}}{15}\right)^{\frac{1}{3}}\left(\frac{T_\star}{150\ \mathrm{MeV}}\right)$$

$$H_\star^2 = \frac{8\pi G}{2}\mathcal{E}_{\mathrm{rad},\star} \qquad \mathcal{E}_{\mathrm{rad},\star} = \frac{\pi^2 g_\star}{30}T_\star^4 \qquad (c = k_B = \hbar = 1)$$

$$f_H \simeq (1.8\times10^{-8}\mathrm{Hz})10^{12}\left(\frac{g_\star}{15}\right)^{\frac{1}{3}}\left(\frac{T_\star}{150\ \mathrm{MeV}}\right)$$

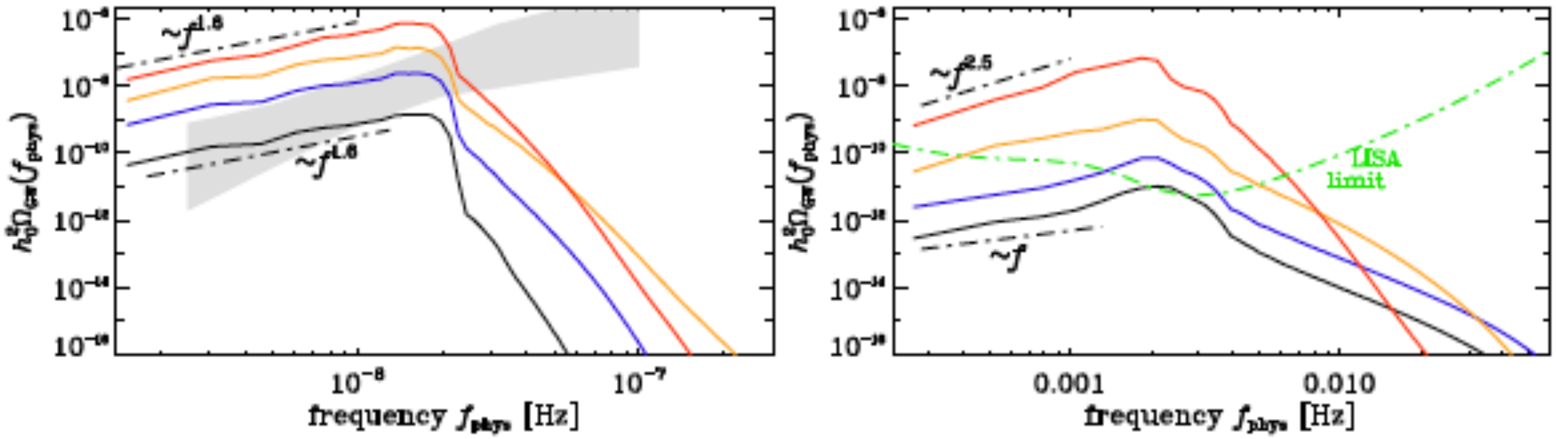

FIG. 2: Frequency spectra, $h_0^2\Omega_{\rm GW}(f)$, for both the QCDPT Runs a–d (left) and the EWPT Runs A–D (right) shown in red, orange, blue, and black, respectively.

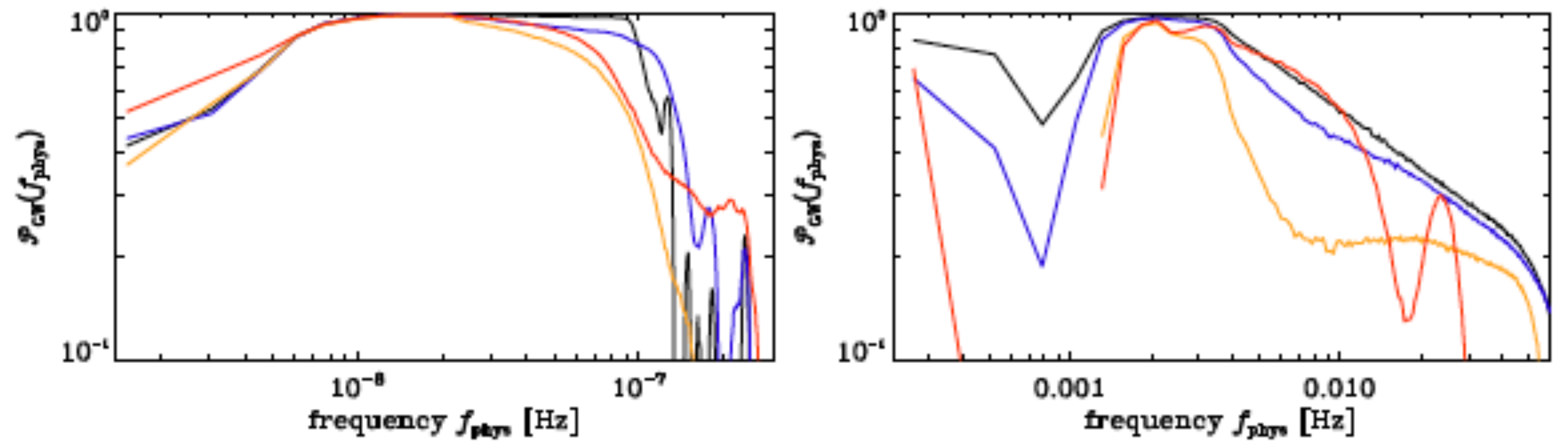

FIG. 3: Polarization spectra, $\mathcal{P}_{\rm GW}(f)$, for the QCDPT Runs a–d (left) and the EWPT Runs A–D (right) [56] shown in red, orange, blue, and black, respectively.

Kahniashvili et al. 2021

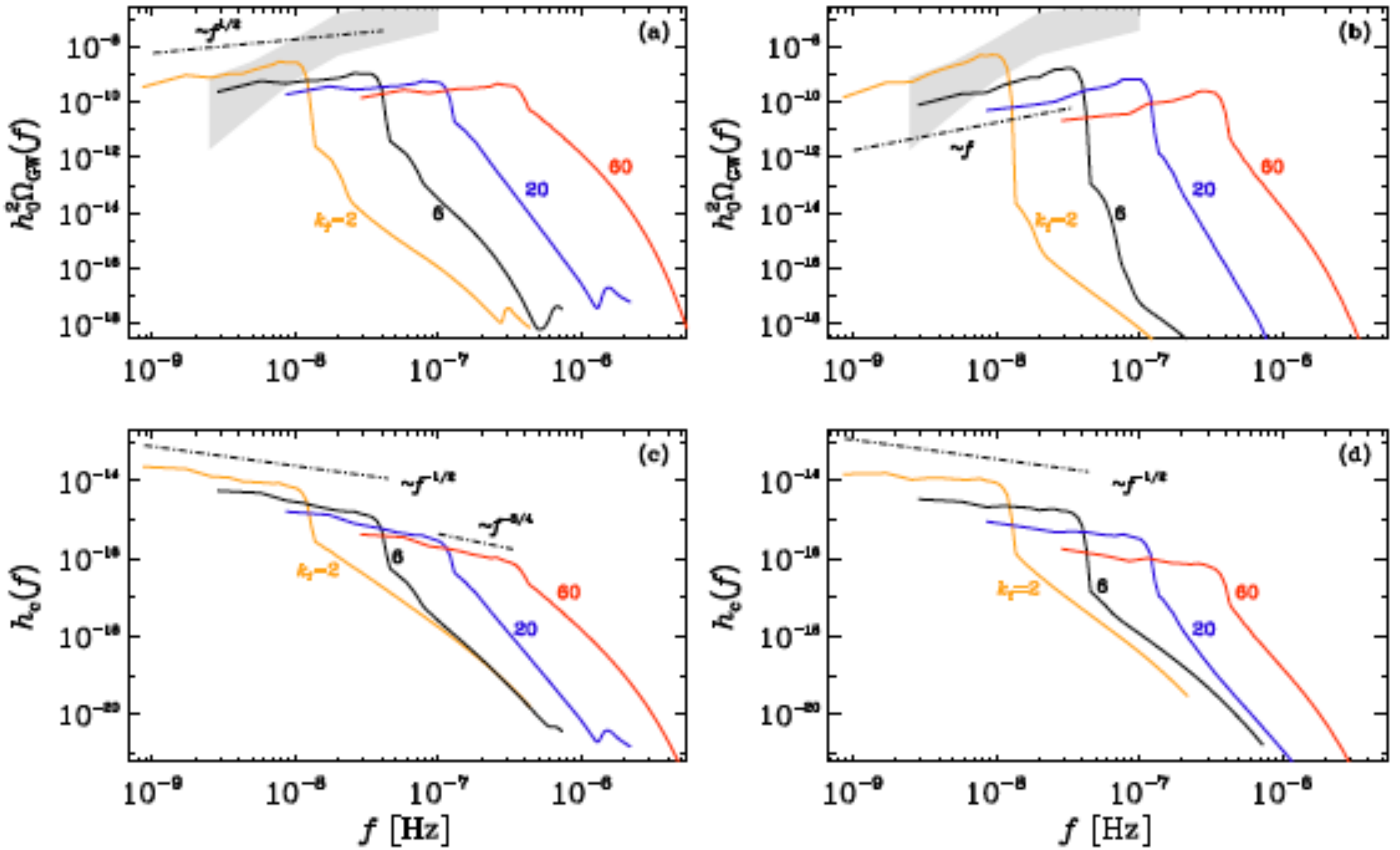

FIG. 5: (a,b) $h_0^2\Omega_{\rm GW}(f)$ and (c,d) $h_c(f)$ at the present time for all four runs presented in Table I, for the (a,c) nonhelical and (b,d) helical runs. The 2σ confidence contour for the 30-frequency power law of the NANOGrav 12.5-year data set is shown in gray.

Brandenburg et al. 2021

Gravitational Waves Missions

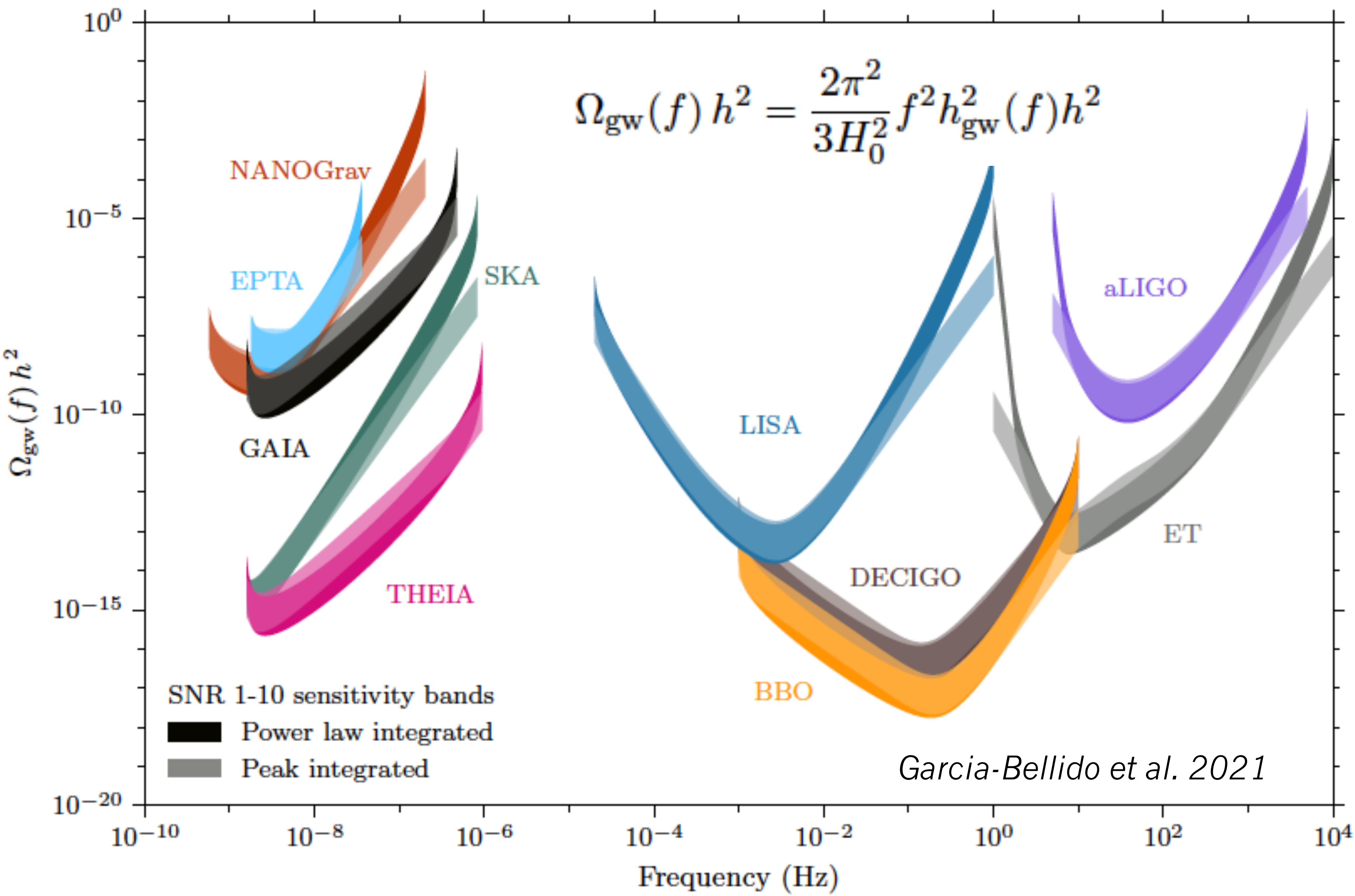

Take Home Comments

- Improve the Magnetic Fields Observations in Voids and Filaments
- Advance Numerical Simulations Technique to Model Primordial Magnetic Fields and Turbulence
- Determine the mechanisms insuring the presence of viable magnetic field/turbulent sources in the early universe and correspondingly correct initial conditions:
  - Primordial magnetogenesis
  - Bubble collisions/nucleation – more realistic models
  - Sound waves as a source for turbulence
  - Axions driven turbulence and axion like particles driven inflationary new physics
  - Cihiral sources and gravitational waves polarization

Acknowledgements:

- **Workshop Organizers:** Franco Vazza, Daniela Paoletti, Fabio Finelli, Elisa Prandini
- **Collaborators:** Axel Brandenburg, Emma Clarke, Grigol Gogoberidze, Youtong He, Arthur Kosowsky, Andrew Long, Sayan Mandal, Deyan Mihaylov, Matthias Rheinhardt, Alberto Roper Pol, Jennifer Schober, Nakul Shenoy, Jonathan Stepp, Guotong Sun.
- **Support from:** GNSF (FR18-1462), NASA ATP (80NSSC22K0825), Swedish Research Council (2019-04234),

Thank You